ASSESSING THE ROLE OF HIGH AFFINITY SORPTION SITES IN CESIUM DESORPTION FROM HYPERALKALINE-WEATHERED HANFORD SEDIMENTS

by

YI-TING DENG

(Under the Direction of Aaron Thompson)

ABSTRACT

At the Department of Energy's Hanford Site, hyperalkaline (pH > 13) and radioactive waste leaking from storage tanks causes rapid sediment weathering and *de novo* mineral formation—both of which can alter the mobility of the principal radioactive contaminants, Cs and Sr. These new-formed minerals, such as NO_3-feldspathoids, sequester contaminants in their structures and the frayed-edge sites (FES) of the sediment clays strongly bind Cs. However the long-term stability of the sequestered contaminants is unknown, so existing reactive-transport models cannot address weathering related impact of the sediments. Our goal is to determine the mechanisms of contaminant release from NO_3-feldspathoids and to quantify how the weathering process alters the FES density. Our results suggest that Cs and Sr are released from NO_3-feldspathoids through both ion exchange and mineral dissolution. Furthermore, the hyperalkaline-weathering process increases the density of high-affinity Cs sorption sites in Hanford sediments, which may include the FES and also the high-affinity sites on the neo-formed minerals.

INDEX WORDS: Cs Release, Sr Release, NO_3-Feldspathoids, Ion exchange, Mineral Dissolution, Frayed-Edge Sites (FES) Density.

ASSESSING THE ROLE OF HIGH AFFINITY SORPTION SITES IN CESIUM DESORPTION FROM HYPERALKALINE-WEATHERED HANFORD SEDIMENTS

by

YI-TING DENG

B.S., National Chung Hsing University, Taiwan, 2008

A Thesis Submitted to the Graduate Faculty of The University of Georgia in Partial Fulfillment of the Requirements for the Degree

MASTER OF SCIENCE

ATHENS, GEORGIA

2012

ASSESSING THE ROLE OF HIGH AFFINITY SORPTION SITES IN CESIUM DESORPTION FROM HYPERALKALINE-WEATHERED HANFORD SEDIMENTS

by

YI-TING DENG

Major Professor: Aaron Thompson

Committee: David Radcliffe
John C. Seaman
Paul A. Schroeder

Electronic Version Approved:

Maureen Grasso
Dean of the Graduate School
The University of Georgia
May 2012

DEDICATION

I would like to dedicate this thesis to my mother, who had always believed in me before she passed away. It is her love that has supported me through every difficulty I have met.

ACKNOWLEDGEMENTS

I would like to thank Dean Angle for providing the research assistantship, and thank my major advisor as well as other committee members for advising me on my research and the pursuit of a future career. I would also like to thank John Rema for NO_3 analysis, Gene Weeks for ICP-MS analysis, John Shields for TEM analysis, and all the lab-mates for the research assistance. Last but not least, I thank my family, especially my father and my fiancé for the support during my Master's study.

TABLE OF CONTENTS

Page

LIST OF TABLES

Page

LIST OF FIGURES

Page

CHAPTER 1

INTRODUCTION

1.1 Literature Review

The Department of Energy's Hanford Site covers 1517 km^2 in southern-central Washington State, and the Columbia River flows along the site for 80 km. During World War II, the Hanford Site was selected to produce plutonium (Pu), one of the vital radionuclides for nuclear weapons. As a result, huge volumes of radioactive and chemical wastes were generated from the reprocessing of spent nuclear fuel from 1943 to 1989. These wastes were stored or discharged based on their characteristics and potential hazards. Some of the most hyperalkaline-radioactive (pH>13) wastes were stored in 177 single- and double-shelled, carbon-steel tanks that were originally built to last for at least 500 hundred years; however, leaks from single-shelled tanks were suspected in 1956 and confirmed in 1959 (1). It is difficult to determine the exact volume of tank waste loss, but over 5,500 million m^3 were leaked, containing a total of ~1,500,000 curies of radioactivity (2). This finally led to the largest environmental cleanup project in the U.S. due to the complexity and extent of hyperalkaline-radioactive contamination at the Hanford site.

The leaking waste has contacted the surrounding sediments for decades and driven several geochemical and radiological transformations (2, 3). For instance, the contact of Hanford sediments and hyperalkaline-radioactive waste promotes the

formation of new minerals; most of them are NO_3-feldspathoids and zeolites (4-6). The primary radionuclide contaminants in the tank waste are ^{137}Cs, ^{90}Sr, and ^{129}I. These contaminants are hazardous because of their high radioactivity. That is why their transport behavior in the sediments beneath the tanks has become an important research subject (7-11), and reactive-transport models have been developed to simulate the transport of these contaminants in hyperalkaline-weathered Hanford sediments (12-15).

One of the difficulties in characterizing the transport of these radioactive contaminants is that the existing reactive-transport models used to simulate the Hanford Site contamination do not adequately address the impact of this *de novo* mineral formation. It is known that NO_3-feldspathoids can incorporate the contaminants (Cs, Sr) and their accompanied anion NO_3 in the mineral framework (Figure 1.1), which emphasizes the need to understand the mechanisms of Cs and Sr release from these neo-formed minerals (16, 17). Few studies of Cs and Sr release from hyperalkaline-weathered Hanford sediments containing the neo-formed minerals have been reported (14, 16, 18-20). Previous studies have found that ion exchange and mineral dissolution are two major mechanisms of controlling the Cs and Sr transport in hyperalkaline-weathered Hanford sediments. Thompson et al. (2010) suggested that Cs release from NO_3-feldspathoid is via ion exchange, but Sr and NO_3 desorption could be via NO_3-feldspathoid dissolution (14). However, due to the limited leaching period, the long-term fate of the $CsNO_3$ or $Sr(NO_3)_2$ component in NO_3-feldspathoids and the mechanism of long-term release from hyperalkaline-weathered Hanford sediments still remain unclear.

We hypothesize that the mechanism could be determined by a long-term leaching of hyperalkaline-weathered Hanford sediments containing NO_3-feldspathoid.

Additionally, it is known that there are three cation sorption sites on clay minerals that occur in the sediments (Figure 1.1), including planar sites (regular exchange sites), frayed-edge sites (wedge-shaped zones), and collapsed or hydrated interlayer sites (21). Compared to planar sites or other interlayer sites, the frayed edge sites (FES), wedge-shape zones between expanded and non-expanded layer, have lower capacity but higher sorption affinity for Cs (22-24). Many studies have shown that FES can control Cs sorption in 2:1 clay minerals (2, 13, 15, 22, 25, 26). Therefore, it is important to estimate the contribution of FES to Cs sorption in order to predict Cs transport and the mechanisms of Cs release from clay minerals. The silver thiourea (AgTU) method is commonly used method to measure the FES density of clay minerals. This method uses the AgTU complex to block planar sites, restricting Cs sorption on FES of the layer silicates (27). The [FES-Cs] is calculated as the difference between the initial Cs and the remaining Cs in the solution. However, Zachara et al. (2002) proposed that AgTU may not effectively block the planar sites, which would result in over-estimation of FES density (15). Furthermore, only the FES density of the uncontaminated Hanford sediments has been characterized (13, 15). The FES density of waste-contacted Hanford sediments, which have been weathered under hyperalkaline conditions that result in mineral dissolution and precipitation of neo-formed zeolite and feldspathoid phases, may be considerably different. Previous studies have proved that mineral transformation can alter the FES or other high-affinity Cs

sorption sites, and further alter the behavior of Cs sorption (7, 28-30). However, the impact of weathering process (i.e., the formation of neo-formed minerals) on altering the density of FES and other high-affinity Cs sorption sites of hyperalkaline Hanford sediments has not been well studied.

1.2 Research Objectives

Our research has the following three objectives: (1) to determine the mechanism of Cs and Sr release from NO_3-feldspathoids by tracking the loss of their accompanied anion NO_3^- using the three-month leaching technique; (2) to evaluate techniques for measuring FES density and determine the most suitable method to apply on hyperalkaline-weathered Hanford sediments; and (3) to directly measure the density of FES and other high-affinity Cs sorption sites of hyperalkaline-weathered Hanford sediments by using two methods: AgTU method and flow-through technique, and to further estimate the impact of hyperalkaline weathering on Cs sorption in Hanford sediments. The mineral quantification work was conducted by Nicolas Perdrial at the University of Arizona (6).

1.3 Thesis Format

This thesis contains five main chapters and appendices, including Chapter 1 – Overall introduction; Chapter 2 – The mechanism of contaminant and NO_3 release from NO_3-feldspathoids; Chapter 3 – The evaluation of techniques for measuring FES density of pristine Hanford sediments; Chapter 4 – The alteration of high-affinity cesium sorption

sites of hyperalkaline-weathered Hanford sediments; Chapter 5 – Overall conclusions. The appendices contain the characterization of hyperalkaline-weathered Hanford sediments, the mineral formation of Hanford sediments under different weathering conditions, the release of cations from hyperalkaline-weathered Hanford sediments containing most zeolites, and the FE-SEM image and EDS-spectra of Hanford sediments saturated with different cations.

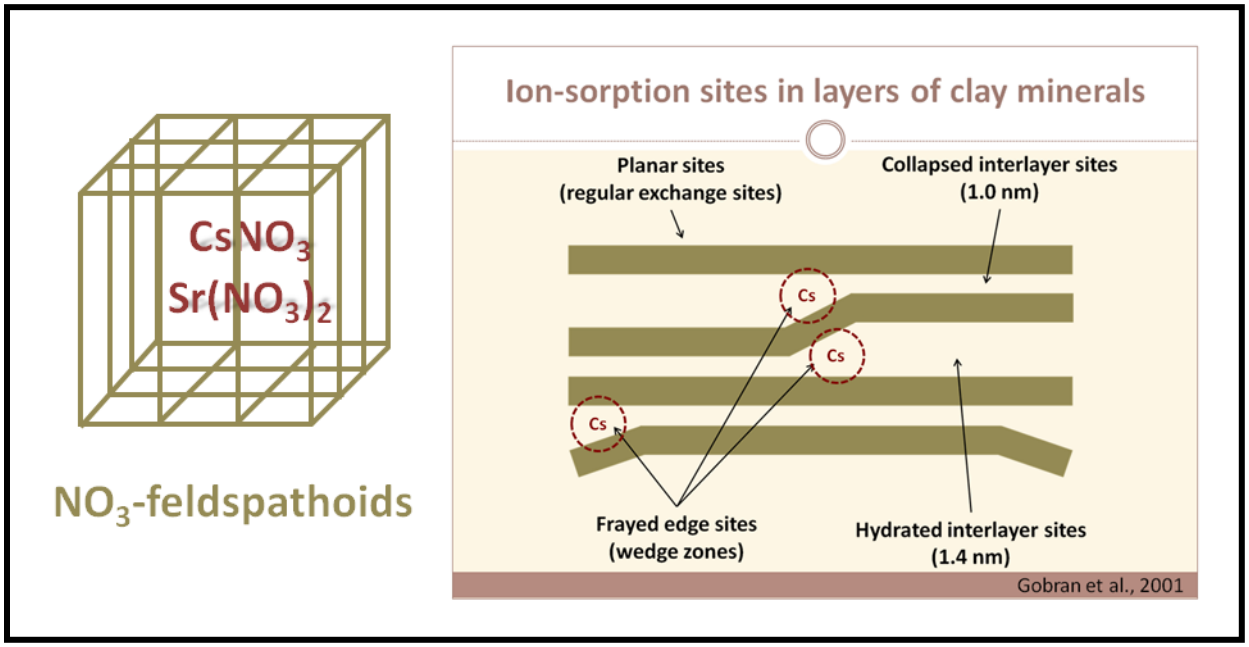

Figure 1.1. Cs, Sr and NO_3 trapped in NO_3-feldspathoids and Cs on the FES in clay minerals. $CsNO_3$ and $Sr(NO_3)_2$ in this figure stand for Cs-NO_3 or Sr-$(NO_3)_2$ ion pairs.

CHAPTER 2

CONTAMINANTAND NITRATE DESORPTION DURING THREE-MONTH LEACHING OF HYPERALKALINE-WEATHERED HANFORD SEDIMENTS[1]

[1] Deng, Y.T., N. Perdrial, A. Thompson. To be submitted to Environmental Science & Technology.

Abstract

The contact of hyperalkaline radioactive waste with Hanford sediments at Department of Energy's Hanford Site causes the formation of neo-formed minerals, including NO_3-felspathoids and zeolites that are known to incorporate the contaminant Cs and Sr into their structures. Cs and Sr are expected to reside as ion-pairs with NO_3 in the internal cages of NO_3-feldspathoids. The long-term stability of Cs and Sr thus depends not only on the solubility of the host mineral phase, but also the susceptibility of the $CsNO_{3(aq)}$ or $Sr(NO_3)_{2(aq)}$ ion pairs to exchange reactions. We elucidated the relative importance of ion exchange and neo-formed solid dissolution on net Cs and Sr release by leaching hyperalkaline-weathered Hanford sediments rich in NO_3-felspathoids for three months (~8000 pore volumes) and tracking the loss of Cs^+,Sr^{2+}, NO_3^-, and the net change in the abundance of feldspathoid phase. Our results show that the ratio of the remaining NO_3 to the remaining NO_3-felspathoids ranges from 0.028-0.071 of the LOW treatments containing NO_3-feldspathoids before leaching, while it is all within the range of 0.025-0.033 after the ~8000 PV leaching. This suggests that during leaching Cs and Sr are released initially as ion-pairs until the mass ratio of remaining NO_3 to remaining NO_3-feldspathoids reaches ~ 0.025. After that point, NO_3 release coincides with the dissolution of the NO_3-feldspathoid mineral. However, the reactive-transport modeling suggests that Cs release from sediment-bound NO_3-feldspathoids occurs primarily via ion-exchange and the frayed-edge sites control long-term Cs release. This may suggest that partial Cs release from FES is decoupled with NO_3 release. Finally, a stable molar

stoichiometry of NO_3 in NO_3-feldspathoids ranging from 0.408 to 0.541 is observed after ~8000 PV leaching.

2.1 Introduction

The Department of Energy's Hanford Site is the most radioactively contaminated site in the United States, and a significant amount of research has been conducted basing on its complex hyperalkaline-radioactive contamination (9, 13-15, 18, 19, 31-34). The hyperalkaline-radioactive waste has contacted the surrounding vadose zone sediments for decades, resulting in geochemical and radiological transformations (2, 3, 35, 36). According to previous research, Zeolites (chabazite-type) and NO_3-feldspathoids (sodalite and cancrinite) are two major neo-formed minerals in the hyperalkaline-weathered Hanford sediments, but their relative amounts depend on the sediment weathering conditions (20). It is also known that these neo-formed solid phases can incorporate Cs and Sr into the mineral structure (16, 18, 19). For example, $CsNO_{3(aq)}$ or $Sr(NO_3)_{2(aq)}$ may exist as ion-pairs in NO_3-feldspathoids, which formation is promoted by hyperalkaline and high ionic-strength waste (4, 5, 35). Many studies have been conducted to describe contaminant behavior in the hyperalkaline Hanford weathered sediments, especially on the transport of Cs and Sr (7, 12, 13, 15, 22, 31, 37-39), but few of them have focused on the long-term fate and mechanisms of Cs and Sr release from these neo-formed minerals. This hampers application of existing reactive-transport models to the Hanford Site, as most model do not adequately incorporate interactions between contaminants and the neo-formed minerals.

The mechanisms of Cs and Sr release from the neo-formed minerals have been the subject of several recent studies. In 2005, the work from Mon et al. (16) suggested that only 15% of Cs in sodalite and 22-57% of Cs in cancrinite was exchangeable with Na^+, K^+ and Ca^{2+}, while 94-99% of Cs in zeolite and allophone was exchangeable with Na^+ and K^+. In 2008, the dissolution kinetics studies of Chorover et al. (19) suggested that remobilization of the sequestered Cs^+ and Sr^{2+} in hyperalkaline-weathered Hanford sediments may occur without extensive mineral dissolution, depending on the cation concentration and type (e.g. Ca^{2+} and K^+) in the soil solution. Their results indicated that co-precipitation and ion exchange in neo-formed minerals may be an important mechanism controlling Sr^{2+} and Cs^+ mobility, but an improved understanding of contaminant remobilization in the Hanford background pore water is necessary to predict the long-term fate of Cs^+ and Sr^{2+} in the Hanford sediments. McKinley et al. (9) also proposed that $^{90}Sr^{2+}$ mobility could be controlled by cation exchange and $CaCO_3$ solubility in the vadose zone. In 2010, Thompson et al. (14) leached hyperalkaline-weathered Hanford sediments containing NO_3-feldspathoids for ~ 600 pore volumes and found that Cs, Sr and NO_3 were released when they were exposed to the Hanford background pore water. Their result suggests that Cs release could be modeled via ion exchange, but Sr and NO_3 release was assumed to derive from NO_3-feldspathoid dissolution. However, due to the limited leaching period, the long-term fate of Cs, Sr and NO_3 in NO_3-feldspathoids and the mechanism of their long-term release still remain unclear.

Thus, our goal was to elucidate the mechanism of contaminant (Cs and Sr) and NO_3 release from NO_3-feldspathoids in the hyperalkaline-weathered Hanford sediments. Specifically, we hypothesized that the mechanism of Cs and Sr release could be determined by tracking the loss of their accompanied anion NO_3^- and the dissolution of NO_3-feldspathoids. If there is no NO_3-feldspathoids remaining after the exhaustive leaching of NO_3, it suggests that mineral dissolution controls both contaminant and NO_3 release. If NO_3-feldspathoids remain after the exhaustive leaching of NO_3, it suggests that ion-exchange controls the contaminant and NO_3 release. To test this hypothesis we conducted a ~8000 PV leaching of reacted Hanford sediments to remove the majority of NO_3^-. Perdrial et al. (6) provided the solid phase characterization of hyperalkaline-weathered sediments, and we analyzed the abundance of feldspathoid phases in the leached sediments via quantitative x-ray diffraction (XRD). This allowed us to quantify NO_3-feldspathoid dissolution after the ~8000 PVs leaching.

2.2 Materials and Methods

2.2.1 Sediment Collection and Contamination

Sediments were collected from an uncontaminated area within the Hanford formation; specifically, the 218-E-12B Burial Ground excavation site (40). The sediments have similar characteristics (Appendix A) to those beneath the leaking tanks at the DOE Hanford Site. Sediments were air dried, and sieved to obtain the less than 2 mm fraction. Contamination of the pristine Hanford sediments was simulated with either low concentrations [LOW] of Sr, Cs and I (10^{-5}, 10^{-5}, and 10^{-7} molal) or high concentrations

[HIGH] of Sr, Cs and I (10^{-3}, 10^{-3}, and 10^{-5} molal) present in hyperalkaline Na-Al-NO_3-OH solution (synthetic tank waste leachate or STWL), which is known to promote rapid, incongruent silicate weathering and feldspathoids formation. STWL contains 0.05 M $NaAlO_2$, 2.0 M Na^+, 1.0 M NO_3^-, and 1.0 M OH^- (pH 13.7). The experimental conditions used by Chorover and his co-workers (18, 41-43) were modified in this work.

Sediments were reacted in 20-L acid washed, polypropylene co-polymer (PPCO) carboys containing 400 g of air-dried sediments in 20 kg of STWL. The sediments and STWL were reacted for either 6 months [6 mon] or 12 months [12 mon] in (1) CO_2-free conditions [-CO_2] (< 10 ppmv pCO_2) or (2) atmospheric CO_2 conditions [+CO_2] (385 ppmv pCO_2). The carboys were manually shaken once per day for five out of seven days of the week. Finally, the sediments were separated from the solution by centrifugation at 27,257g for 45 minutes and washed three times by 95% ethanol followed by a final wash with reagent grade water. The collected sediments were freeze-dried, homogenized, and stored at 25°C. More details provided in Thompson et al (14).

2.2.2 Column Experiments

Approximately 1.8 g of pristine or reacted Hanford sediments were packed into 0.6547 cm I.D. X 2.1 cm long (pack length) non-fluorous polypropylene columns, yielding an average porosity of $0.520_{\pm 0.004}$. The columns were leached continuously at a uniform flow rate (~0.05 mL min^{-1}) with Hanford background pore water for three months corresponding to ~8000 PVs. Hanford background pore water contains (mg L^{-1}): 210.38 NaCl, 8.40 $NaHCO_3$, 22.37 KCl, 231.44 $CaSO_4$, 183.05 $CaCl_2 \cdot 4H_2O$, 203.30

$MgCl_2 \cdot 6H_2O$. All the chemicals were placed in 1 L PPCO bottles, shaken for 30 min, and bubbled with air using a plastic pipet for 12 hr. The solution pH was adjusted to 7.2 with 0.1 M NaOH, and air was bubbled again for an additional 30 minutes and the pH was readjusted to 7.2. This procedure was repeated until the pH was stable. Final solution molarities were: 3.6 mM NaCl, 0.1 mM $NaHCO_3$, 0.3 mM KCl, 1.7 mM $CaSO_4$, 1.0 mM $CaCl_2$, 1.0 mM $MgCl_2$. Effluents were collected in 250 mL acid-washed PPCO bottles every 72 hr for 3 months, yielding around 8000 PVs in the end for each column. The bottles were capped and frozen at -20°C immediately after collection.

2.2.3 Column Experiment Analysis

At the time of analysis, effluents were shaken thoroughly after thawing in capped bottles. Then, the effluents were diluted for pH measurement, NO_3 analysis via nitrogen analyzer (Alpkem, RFA-300), and analysis of Ca, Mg, K, Na, Cs, Sr, I and Si via inductively coupled plasma mass spectrometry (ICP-MS) (Perkin-Elmer, Elan 9000) and atomic absorption spectroscopy (AA) (Perkin-Elmer, AAnalyst 200).

2.2.4 Reactive-Transport Modeling

In previous modeling work (13, 14), the reactive transport code Crunchflow (www.csteefel.com) was used to simulate the dissolution, precipitation, and transport of Cs and Sr in hyperalkaline-weathered Hanford sediments for column experiments. The multicomponent reactive transport equation used in the CrunchFlow was:

$$\frac{\partial(\phi Ci)}{\partial t} = \nabla \bullet (\phi DiCi) - \nabla \bullet (\phi uCi)$$

where ϕ is the porosity (0.52 in this research), C is the concentration of the ith primary species, D is the dispersivity coefficient (0.04 M in this research), u is the velocity

vector. More detail about the equation was provided in Dontsova et al. (44). The main modeling work in this study is to improve the input parameters of those existing models through the experimental measurements from this research to help determine the mechanism of Cs release. The same model construction in Thompson et al. (14) was used in this research to examine the potential for release of Cs via ion exchange. The Cs desorption of 6 month High and Low treatments were modeled by changing the ion exchange parameters (i.e. selectivity coefficient of Cs-K and two FES densities).

2.3 Results

2.3.1 Mineral Formation of Different Treatments

Mineral formation resulting from the weathering of Hanford sediments under different contaminant, CO_2, and length of reaction is discussed in Perdrial et al. (6) (Figure 2.1). The LOW treatments formed sodalite-type material (NO_3-feldspathoids) while the high treatments formed chabazite-type material (zeolites); whereas, [+CO_2] treatments formed calcite while [-CO_2] treatments formed stratlingite-type material. Our work here focuses mainly on the LOW treatments, which formed NO_3-feldspathoids. The quantitative results of NO_3-feldspathoids show that the dissolution of NO_3-feldspathoids happened in the LOW treatments during ~8000 PVs of leaching (Table 2.1). Among all LOW treatments, the [12 month L-C] treatment contained the highest initial NO_3-feldspathoids (50,606 mg kg^{-1} soil) and lost 45% of it the mineral mass during leaching, whereas the [6 month L+C] treatment contained the lowest initial NO_3-feldspathoid concentration (13,621 mg kg^{-1} soil) and experienced only minimal dissolution (9%)

during leaching. The other two treatments, [12 month L+C] and [6 month L-C], had 32% and 48% of NO_3-feldspathid dissolution, respectively.

2.3.2 NO_3 Release

Compared to the LOW treatments, the HIGH treatments contained a relatively small amount of initial NO_3 because high contaminant concentrations tend to favor the formation of zeolites, rather than NO_3-feldspathoids (Table 2.1). After ~8000 PVs of leaching, more than 50% of the initial NO_3 was released across all treatments with detectable NO_3 still being released from the four LOW treatments at the end of leaching (Figure 2.2). The LOW treatments [6mon L+C], [6mon L-C], [12mon L+C], and [12mon L-C] released 458.8, 426.4, 593.0, and 517.8 (mg kg^{-1} soil) of total NO_3, corresponding to 67%, 65%, 50%, 51% of total NO_3, respectively. After ~8000 PVs of leaching, the 6-month reacted sediments released ~65% of their total NO_3, compared with 50% of total NO_3 released by 12-month reacted sediments. In addition, all LOW treatments exhibited a transition in the rate of NO_3 release from ~13.0 mg kg^{-1} soil. d^{-1} prior to 2100 PVs to a rate of ~1.8 mg kg^{-1} soil d^{-1} after 2500 PVs. We suspect that this was because the NO_3 amount in the effluents after ~2100 PVs was around the detection limit (0.05 mg L^{-1}).

2.3.3 Cs and Sr Release

The [6-month] HIGH treatments contained more initial Cs than the LOW treatments (Figure 2.3). Except for the [6 mon H-C] treatment, the other three treatments ([6mon L+C], [6mon L-C], [6mon H+C]) all released the majority of Cs and reached a steady state by the end of the ~8000 PV leaching. Both [6 month] LOW treatments released the most of Cs and reached the steady state at ~ 2500 PVs while the [6mon H+C] treatment

released the most Cs and reached the steady state at ~ 4000 PVs (Figure 2.3). By adjusting the selectivity coefficient of Cs-K [(-2.80) to (-2.45)] and densities of FES (FES-1: $3.4*10^{-8}$ µeq g^{-1}, FES-2: $1.5*10^{-7}$ - $2.6*10^{-7}$ µeq g^{-1}) in the CrunchFlow reactive-transport model of Thompson et al. (14), the Cs release from the LOW treatments could be explained solely by ion-exchange reactions. However, the Cs release from the HIGH treatments could not be fit by only changing the above exchange parameters (Figure 2.3). However, unlike Cs, both [6 month] LOW treatments released the majority of Sr and reached the steady state at ~ 1000 PVs (Figure 2.4). The Sr release was greater than Cs release from the LOW treatments (Figure 2.4). Among the 6-month LOW treatments, the [-CO_2] treatment released more Cs than the [+CO_2] treatment before 2000 PVs, whereas the presence of CO_2 did not affect Sr desorption from 6-month LOW treatments (Figure 2.3 and Figure 2.4).

2.3.4 Extension of Cs and Sr Release

In previous studies, Thompson et al. (14) leached the [6 mon L+C] and [6 mon L-C] treatments and Perdrial et al. (in prep.) has leached the [12 mon L+C] and [12 mon L-C] treatments of the reacted sediments for 8 days corresponding to between 500 and 600 PVs. Results from our current work extend the Cs and Sr release from both previous studies (Figure 2.5). Although both Cs and Sr release were still within the detection limit in the end of ~8000 PV leaching, Sr release from the [6-month] and [12-month] treatments reached steady state at ~1000 PVs. However, the extension of Cs release from the [6-month] and [12-month] treatments shows that Cs concentrations were still slowly decreasing at the end of ~8000 PV leaching.

2.4 Discussion

Since Cs and NO_3 or Sr and NO_3 can exist as ion pairs in the NO_3-feldspathoids, the mechanism of $CsNO_{3(aq)}$ or $Sr(NO_3)_{2(aq)}$ release from four LOW treatments can be determined by the ratio of the remaining NO_3 to the remaining NO_3-felspathoids in the sediments after ~8000 PV leaching. If the $CsNO_{3(aq)}$ or $Sr(NO_3)_{2(aq)}$ is released only through mineral dissolution, the ratio of the remaining NO_3 to the remaining NO_3-felspathoids would remain consistent. However, if $CsNO_{3(aq)}$ or $Sr(NO_3)_{2(aq)}$ is released only through ion-exchange, the ratio would decrease over time, inducting of a faster rate of NO_3 release than NO_3-feldspathoid dissolution. The final ratio of the remaining NO_3 to the remaining NO_3-felspathoids of the LOW treatments show release of $CsNO_{3(aq)}$ or $Sr(NO_3)_{2(aq)}$ from the [12 month L-C] treatment is mainly via NO_3-feldspathoid dissolution, while the release of $CsNO_{3(aq)}$ or $Sr(NO_3)_{2(aq)}$ from the [6 month L+C] treatment is mainly via ion-exchange (Figure 2.6). The release of $CsNO_{3(aq)}$ or $Sr(NO_3)_{2(aq)}$ from [12 month L+C] and [6 month L-C] treatments is via both ion exchange and NO_3-feldspathoid dissolution. In addition, the initial ratio of NO_3 to NO_3-felspathoids in the sediments of the [6 month L+C] treatment is 0.071 and that of the [12 month L-C] treatment is 0.028. However, all LOW treatments exhibit similar ratios (0.025 - 0.033 mg mg^{-1}) after ~8000 PV leaching (Table 2.1). This suggests shorter weathering times [6 month] and the presence of CO_2 [+CO_2] generate more exchangeable NO_3. During the leaching, excess NO_3 accumulation above the final stable ratio (~0.025) is lost as ion pairs with a cation (Cs, Sr or other cations). After reaching the stable final ratio 0.025, we predict NO_3 is released only via dissolution of the feldspathoid mineral phase.

Although there has not been direct evidence linking the mechanism of anion release with their specific binding positions inside the feldspathoids, Buhl et al. (45) have found two types of nitrate groups in NO_3-cancrinite, which is one of NO_3-feldspthoids observed in our research. They found the oxygen and nitrogen atoms of both groups can be assigned to different positions in the crystal structure. We hypothesize that these two nitrate groups in different locations may contribute to different release mechanisms. Also, the final ratio of the remaining NO_3 to the remaining NO_3-felspathoids of four LOW treatments is similar across all treatments and suggests a stable stoichiometric composition of NO_3 in the feldspathoids ($Na_8(AlSiO_4)_6$ $(NO_3)_X(Cl)_{2-X}$) in the sediments (Table 2.1). The molar stoichiometry of NO_3 in the feldspathoids of four Low treatments ranges from 0.459 to 1.173 before leaching, while it is within a much smaller range of 0.408 to 0.541 after leaching.

In addition, the recent reactive-transport modeling work performed in previous studies (14, 19, 20) suggests that Cs release is mainly through ion-exchange, which supports the results of modeling work of 6 month LOW treatments in our research. Our modeling work indicates that Cs release from the 6-month LOW treatments during the ~8000 PV leaching can be explained solely by an ion exchange reactive-transport model, and the release after ~2500 PVs can be described by changing the density of two FES (FES-1: $3.4*10^{-8}$ μeq/g, FES-2: $1.5*10^{-7}$ - $2.6*10^{-7}$ μeq/g). This corresponds to the result of release mechanism from the LOW treatments, which releases $CsNO_{3(aq)}$ pair mainly via ion exchange before the final ratio of NO_3 to NO_3-felspathoids reaches 0.025. However, it disagrees with the mechanism of NO_3 release via NO_3-felspathoid

dissolution after this point. This suggests Cs release may be partially decoupled from NO_3 release. A portion of the sorbed Cs is certainly linked to FES cation exchange dynamics and this is not likely to correlate with NO_3 release even during anion exchange. Also, Cs release from the 6-month HIGH treatments after 1000 PVs exceeds the FES exchange capacity of the sediments, so the release after 1000 PVs from the HIGH treatments cannot be fit by only changing FES densities. We hypothesize that Cs release from the HIGH treatments after 2000 PVs involves the mineral dissolution, specifically, zeolite transformation to other minerals (6). Also, by considering the ~8000 PV leaching as an extension of the previous study, Cs is gradually released during the whole long-term leaching from the LOW treatments while Sr release reaches a steady state during the long-term leaching. This suggests that Cs can be slowly released from the FES for a long period. However, Sr does not sorb on FES, which suggests Sr release is either coupled to NO_3 desorption as an ion-pair or via mineral dissolution.

2.5 Conclusions

We found that the ratio of NO_3 to NO_3-felspathoids ranges from 0.028-0.071 of the LOW treatments before leaching, while it is all within the range of 0.025-0.033 after the ~8000 PV leaching. This suggests that $CsNO_{3(aq)}$ or $Sr(NO_3)_{2(aq)}$ can be released from NO_3-feldspathoids first as ion pairs until the ratio of NO_3 to NO_3-felspathoids in the sediments reaches ~0.025. After that, NO_3 and the incorporated Cs and Sr are released mainly via NO_3-felspathoid dissolution. The modeling work suggests that FES-bound Cs

is released via ion exchange and decoupled from NO_3 release during the ~8000 PV leaching.

Table 2.1. The amount of NO_3 and NO_3-feldspathoids, the ratio of NO_3 to NO_3-feldspathoids, and the molar stoichiometry of NO_3 in NO_3-feldspathoids before and after ~8000 PV leaching. The molar stoichiometry is calculated using the molecular weight of NO_3-feldspathoids ($Na_8(AlSiO_4)_6(NO_3)_X(Cl)_{2-X}$).

Treatments		The initial NO_3	The remaining NO_3	Total loss of NO_3	The initial NO_3-feldspathoids	The remaining NO_3-feldspathoids	The initial ratio	The remaining ratio	The initial molar stoichiometry	The remaining molar stoichiometry
		mg kg^{-1} soil	mg kg^{-1} soil	%	mg kg^{-1} soil	mg kg^{-1} soil			(mg mg^{-1})	(mg mg^{-1})
HF	Unreacted	$175_{(5)}$	$71_{(2)}$	60	-	-	-	-	-	-
C1	6mon H+C	$181_{(7)}$	$77_{(2)}$	58	-	-	-	-	-	-
C2	12mon H+C	$492_{(9)}$	$92_{(7)}$	81	-	-	-	-	-	-
C3	12mon L+C	$1362_{(33)}$	$685_{(12)}$	50	$31014_{(1551)}$	$20901_{(1045)}$	$0.044_{(3)}$	$0.033_{(2)}$	$0.726_{(1)}$	$0.541_{(8)}$
C4	6mon L+C	$967_{(13)}$	$321_{(15)}$	67	$13621_{(681)}$	$12358_{(618)}$	$0.071_{(5)}$	$0.026_{(2)}$	$1.173_{(2)}$	$0.429_{(0)}$
C5	12mon H-C	$275_{(2)}$	$77_{(6)}$	72	-	-	-	-	-	-
C6	6mon H-C	$175_{(2)}$	$63_{(3)}$	64	-	-	-	-	-	-
C7	12mon L-C	$1407_{(11)}$	$687_{(16)}$	51	$50606_{(2530)}$	$27820_{(1391)}$	$0.028_{(2)}$	$0.025_{(2)}$	$0.459_{(2)}$	$0.408_{(9)}$
C8	6mon L-C	$924_{(22)}$	$324_{(9)}$	65	$23470_{(1173)}$	$12195_{(610)}$	$0.039_{(3)}$	$0.027_{(2)}$	$0.650_{(6)}$	$0.439_{(1)}$

The subscripts are the standard deviations in concise form [e.g., $1362_{(33)} = 1362 \pm 33$, $175_{(5)} = 175 \pm 5$, $0.033_{(2)} = 0.033 \pm 0.002$].

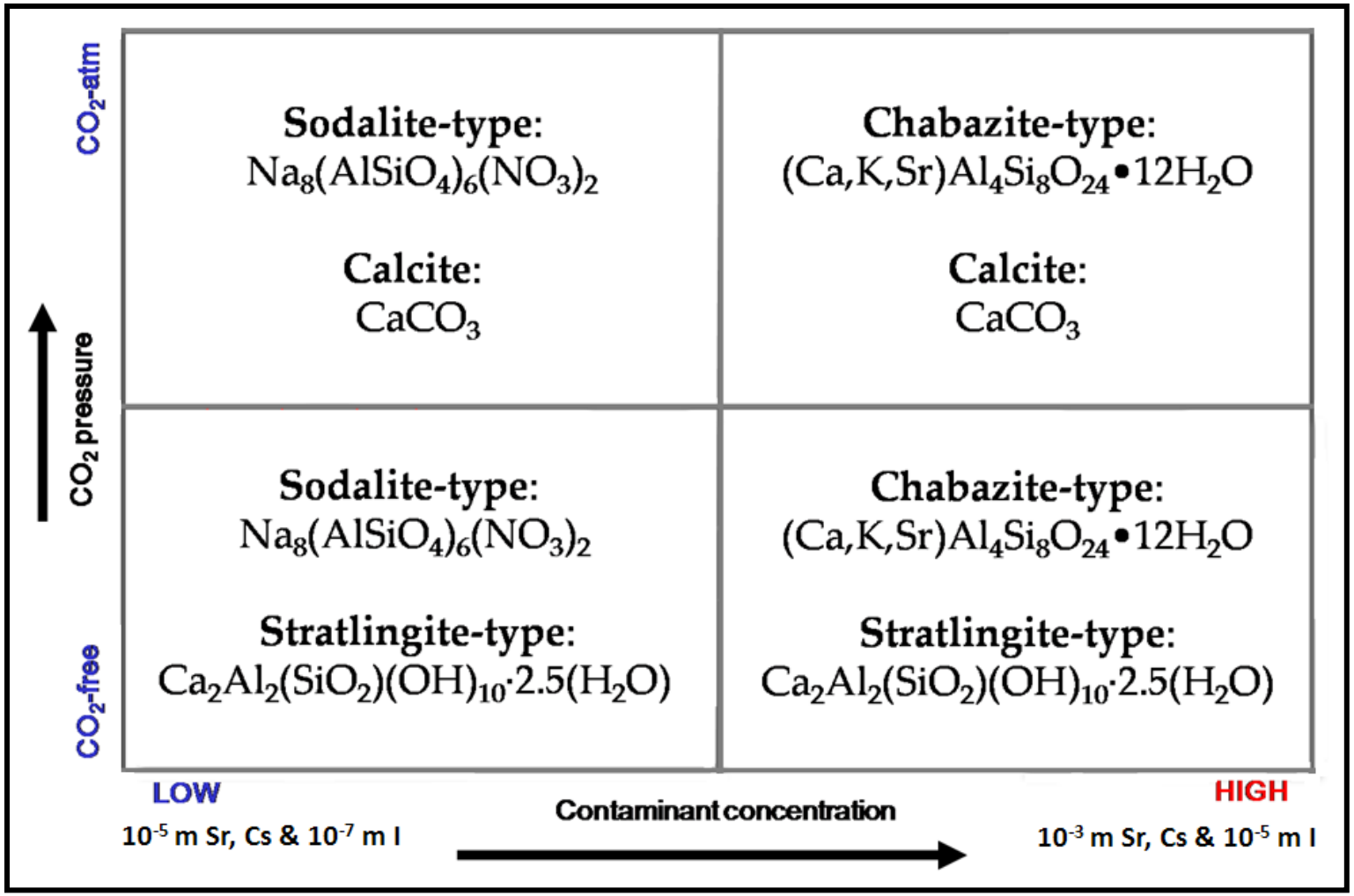

Figure 2.1 Mineral formation under different concentration of contamination, pressure of CO_2, and length of reaction (6).

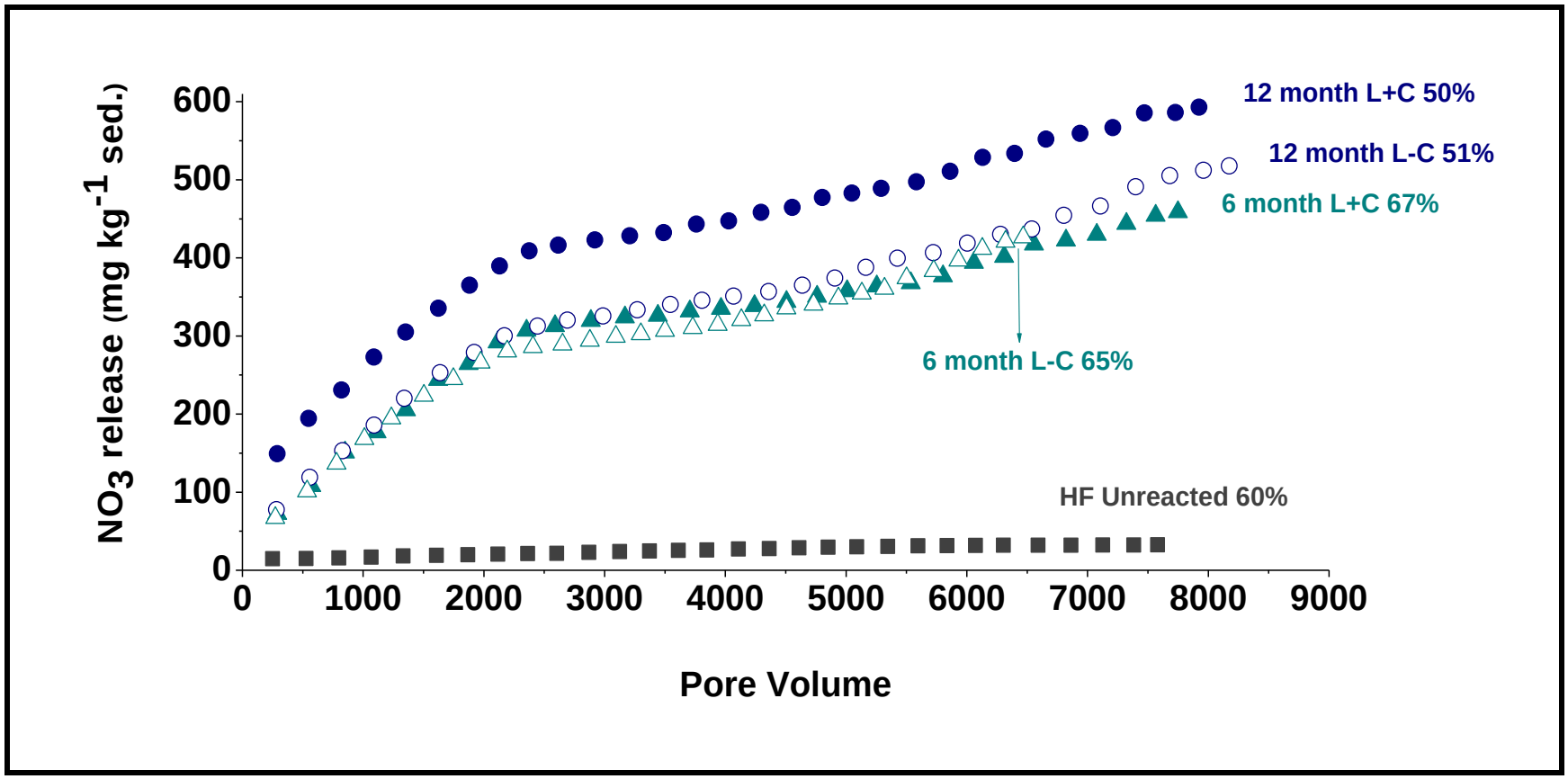

Figure 2.2. Cumulative NO_3 release from the HF unreacted and the four LOW treatments during the ~8000 PV leaching.

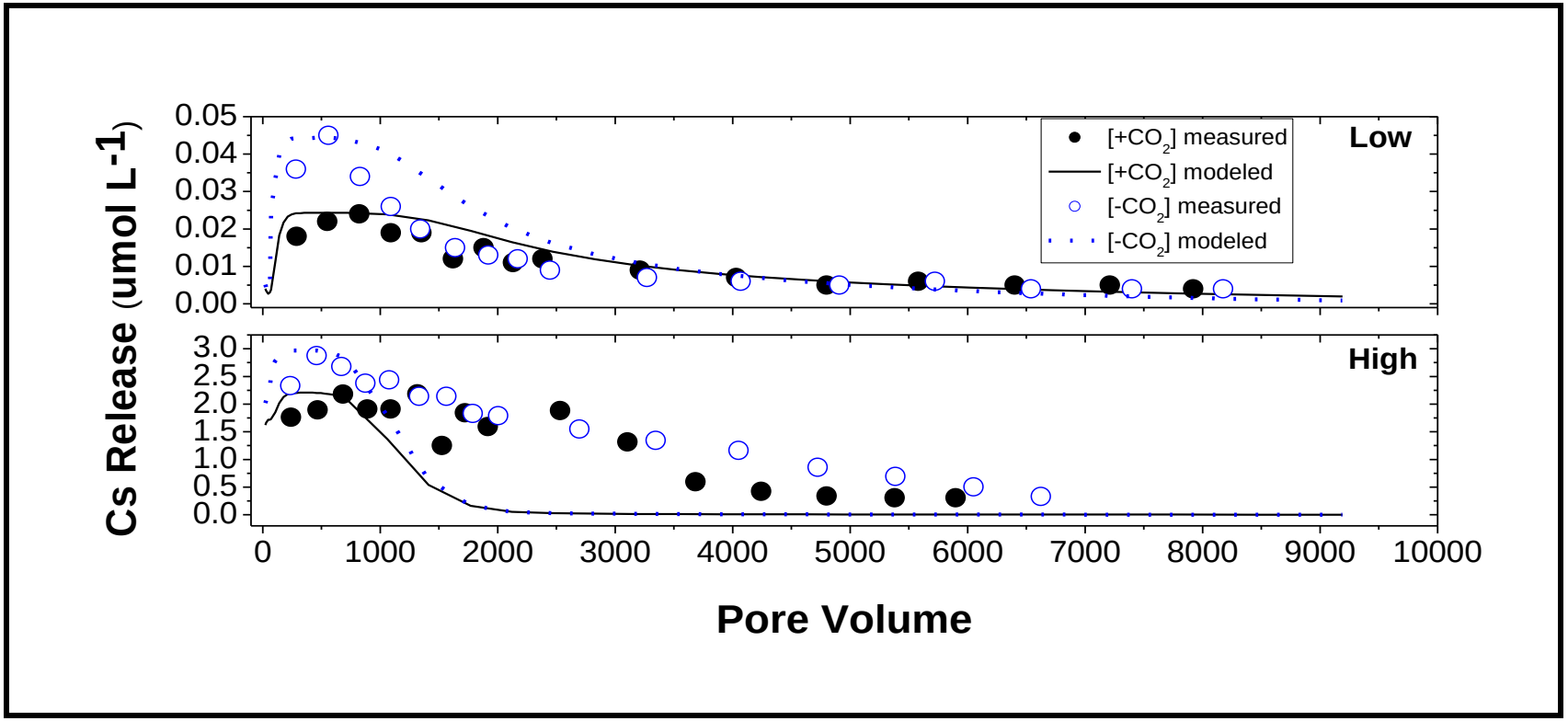

Figure 2.3. Cs release from the 6-month LOW and HIGH treatments during the ~8000 PV leaching.

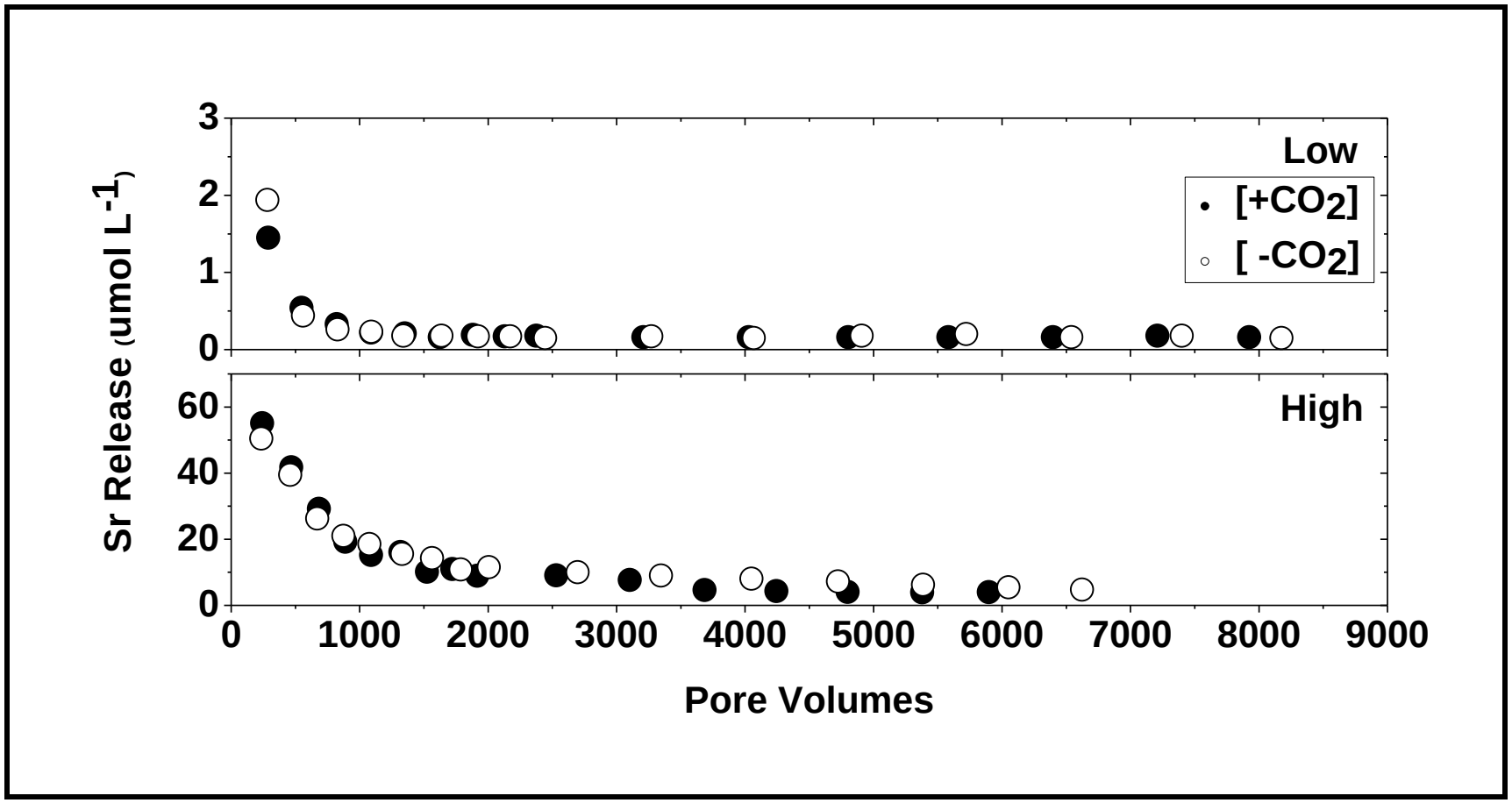

Figure 2.4. Sr release from the 6-month LOW and HIGH treatments during the ~8000 PV leaching.

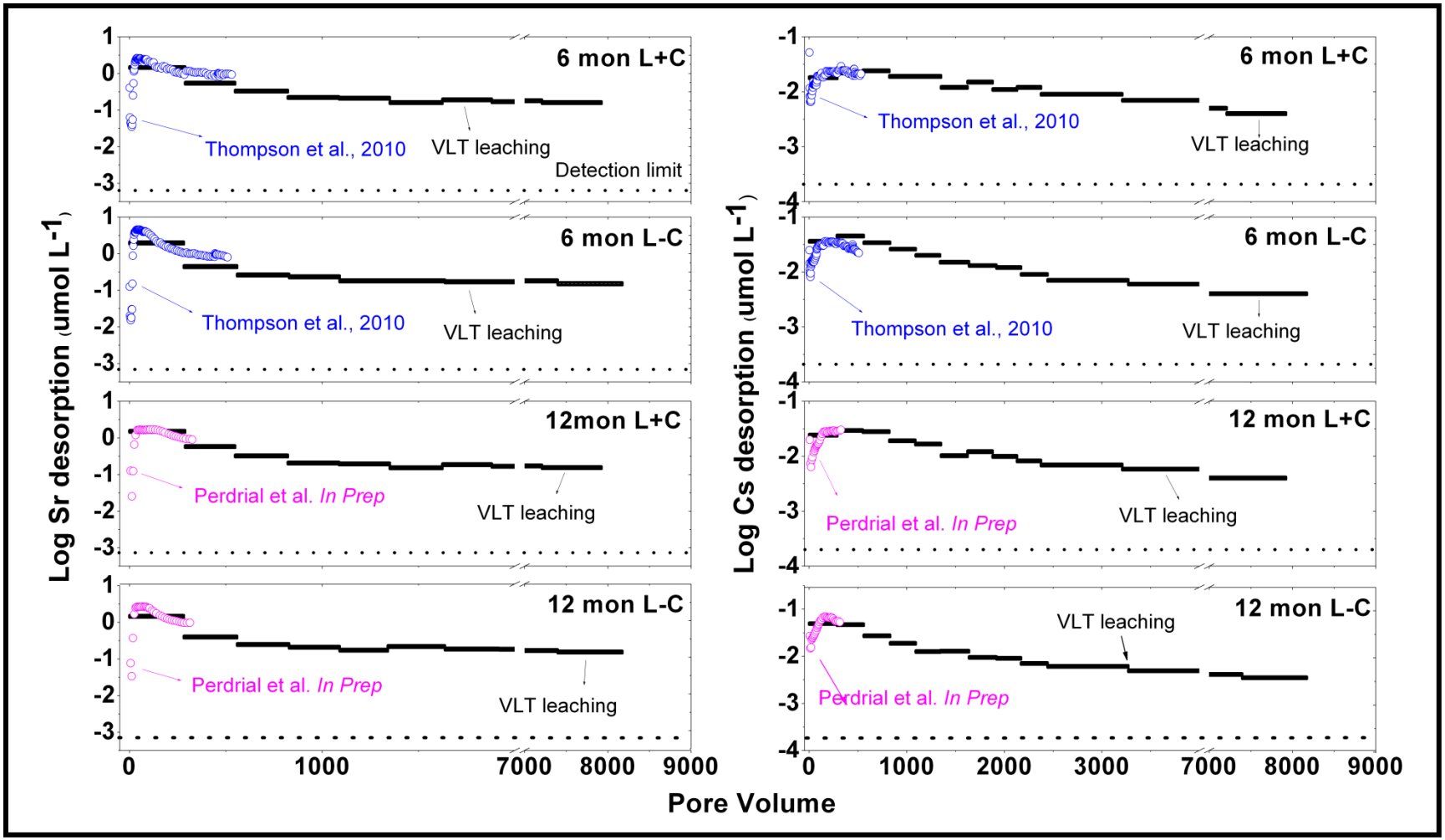

Figure 2.5. The extension of Cs and Sr release from the 6-month and 12-month LOW treatments. VLT leaching stands for Very Long Term (~8000 PV) leaching.

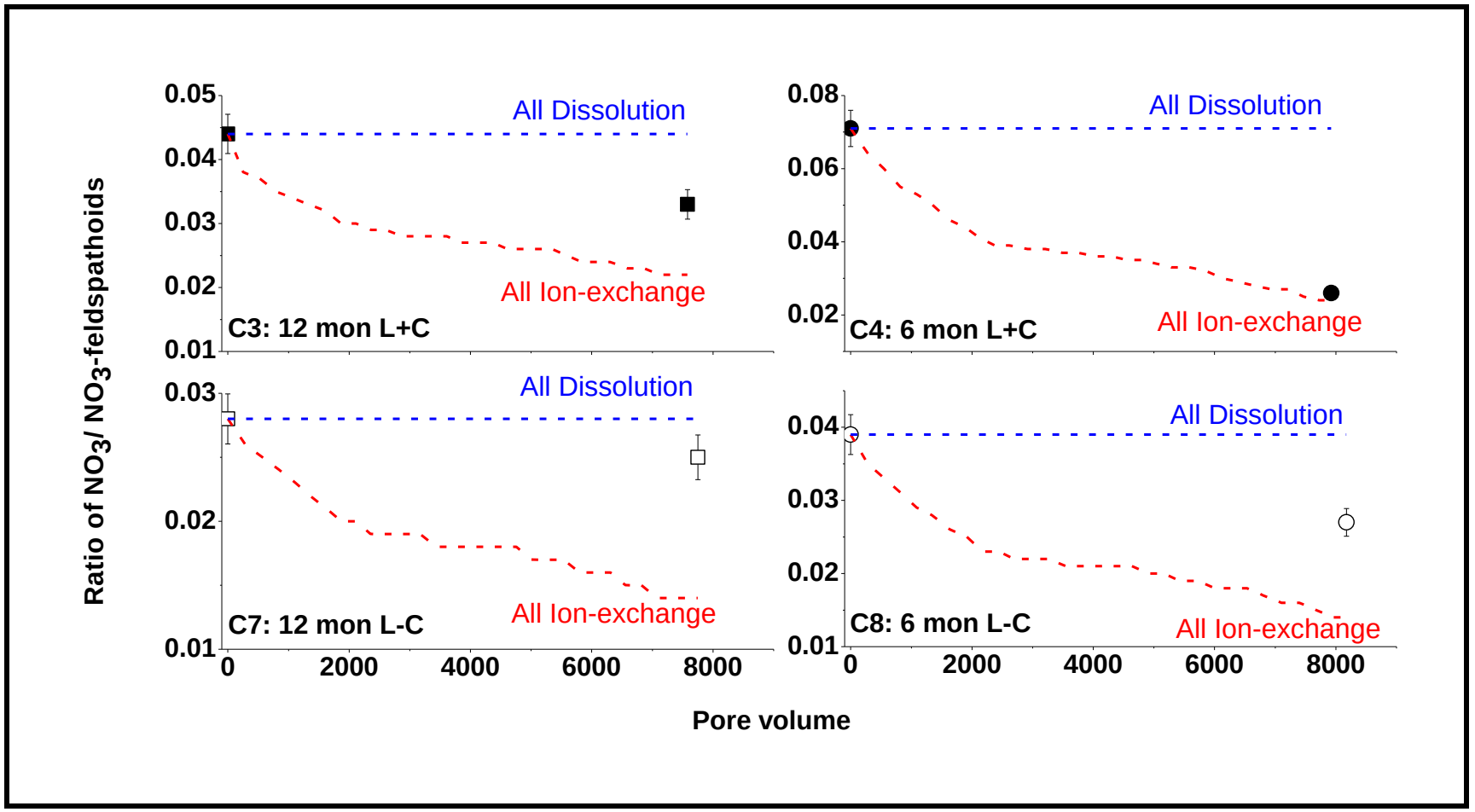

Figure 2.6. Fraction of the concentration of NO_3 to the concentration of NO_3-feldspathoids in the sediments before and after leaching. The dissolution lines represent that NO_3 was released only by NO_3-feldspathoid dissolution. The ion-exchange curves represent that NO_3 was released only by ion exchange, which was calculated based on the remaining NO_3 in the sediments at each sampling point. The symbols represent the ratio of the remaining NO_3 to the remaining NO_3-felspathoids in the sediments before and after ~8000 PV leaching.

CHAPTER 3

EVALUATION OF TECHNIQUES FOR MEASURING THE FRAYED-EDGE SITE OF PRISTINE HANFORD SEDIMENTS[1]

[1] Deng, Y.T., P. A. Schroeder, A. Thompson. To be submitted to Environmental Science & Technology.

Abstract

Frayed-edge sites (FES) are wedge-shaped zones between non-expanded (1.0 nm) and expanded layers (1.4 nm) in micaceous clay minerals. It has been demonstrated that FES have a high affinity for Cs^+ and other poorly hydrated monovalent cations such as K^+, Rb^+, NH_4^+, which can compete with Cs^+ for sorption on FES. Since FES play an important role in Cs sorption, the density of FES on a given clay has become a key parameter of the ion-exchange models used to predict Cs^+ behavior in soils and sediments. Methods for direct measurement of the FES density must discriminate FES from other cation exchange sites. A common method uses the silver thiourea (AgTU) complex to mask planar sites on the clays, allowing Cs to sorb on FES. In this method the [FES-Cs] is calculated as the difference between the initial Cs and remaining Cs. However, it is possible that AgTU may not effectively block the planar sites, and thus excess Cs could sorb to the clay resulting in an over-estimation of the FES density. Our goal is to compare the classical batch AgTU method for estimating FES density with a modified batch AgTU method that includes a desorption step as well as a flow-through column technique that involves sorbing Cs or Rb in the presence of high Ca^{2+} concentrations, which should also block the planar sites. For this evaluation we used pristine sediments from the Hanford Site in Hanford, WA because there is a wealth of existing data of the FES density for these sediments and our ultimate goal is to devise a strategy to measure high-affinity Cs sorption sites when these sediments are contacted with hyperalkaline waste. We also used Rb as an alternative sorptive to evaluate the feasibility of measuring FES density of Cs-containing sediments. The results show that

the AgTU method with the Cs as the sorptive and the flow-through technique with Cs and Rb as the sorptive yield similar FES densities (% of CEC) of pristine Hanford sediments, i.e., 1.19%, 1.37%, and 1.35%, respectively. They are also very consistent with the results of the previous studies. However, the FES density measured from AgTU method using Rb as the sorptive and Modified AgTU method are only 0.68% and 0.11 % of total CEC, respectively. The former is due to insufficient Rb concentration, and the latter is due to over-extraction of Cs^+ by Ca^{2+}. Thus, we concluded that the classical AgTU method and flow-through desorption method with Cs or Rb as the sorptives/sorbates provide satisfactory measurements of the FES density of pristine Hanford sediments at intermediate to high concentrations of Cs. We recommend these methods for measuring the density of high-affinity Cs sorption sites on hyperalkaline-weathered Hanford sediments.

3.1 Introduction

The important role of frayed-edge sites (FES) in the selective sorption of monovalent cations, and particularly those with large ionic radii, such as Cs^+, has been established for over 40 years (24). In micaceous minerals, the frayed-edge sites are wedge-shaped zones between non-expanded (1.0 nm) and expanded layers (1.4 nm), and are known to have much higher affinity for Cs than for cations of higher ionic potential that retain their hydration sphere during sorption. As such, only poorly hydrated monovalent cations such as K^+, Rb^+, and NH_4^+ can compete with Cs to sorb on the FES (46). FES serve as a controlling factor of $^{137}Cs^+$ mobility and availability in

soils because the sorption of Cs in FES can induce the collapse of interlayer sites and further enhance the fixation of Cs (21). For this reason, it is essential to accurately quantify the density of FES in order to predict Cs transport.

The sorption of Cs to the FES of micaceous materials and the exchange selectivity between Cs and other competitive cations has been addressed in many cation exchange models and the FES density is the key parameter in these models (12-15, 22, 46). For instance, Zachara et al. (15) proposed a two-site model (planar site and FES) to describe Cs^+–Na^+, Cs^+–K^+, and Cs^+–Ca^{2+} binary exchange in Hanford sediments, and Steefel et al. (13) added a second FES later to fit the self-sharpening behavior of Cs sorption/desorption at low Cs concentrations. Further, the ion exchange modeling in Thompson et al. (14) suggested that near complete Cs saturation of FES was required before $^{137}Cs^+$ will migrate to planar or interlayer sites; again, suggesting FES provide a central control on the environmental mobility of Cs in soils and sediments. They fit the Cs release curve by altering the initial Cs loading on the exchange sites to 0.032 and 0.029 $mmol_c\ kg^{-1}$ for the Hanford sediments which were contaminated under CO_2-free and atmospheric CO_2 (385 ppmv) conditions, respectively. At these loadings, they suggested that Cs was partitioned almost entirely to the frayed-edge site (FES), and Cs release was governed by K^+ exchange.

Although the importance of FES to Cs sorption is well established, the techniques used to measure FES density are less frequently studied. So far, the silver thiourea (AgTU) method is the most common method for directly measuring the FES density of clay minerals (27). de Koning et al. (27) used the AgTU method to directly

measure the FES density of soils, sediments, and clay minerals. They used 0.015 M AgTU solution to serve as the blocking agent for regular planar sites, and applied $5*10^{-5}$ – $5*10^{-2}$ M $CsNO_3$ in a background of 0.015 M AgTU to sorb Cs on the FES afterwards. After equilibration, Cs adsorption was calculated from the difference between the initial and remaining Cs in the solution. Their measurements of FES density of different pre-treated illites ranged from 2% to 8% of total CEC. However, Zachara et al. (15) found two major problems with the AgTU method. First, they proposed that AgTU-complex did not block all planar sites since the FES density estimated by the isotherm extrapolation procedure in 0.015 M AgTU (FES_{AgTU} = $7.94*10^{-7}$ eq g^{-1}) was significantly higher than that estimated from the multisite modeling ($2.72\text{-}3.45*10^{-8}$ eq g^{-1}). Second, they indicated that Cs was more competitive with AgTU on planar sites of the Hanford sediments than reported on illite, so AgTU was not an effective blocking agent of the planar sites at intermediate to higher Cs concentrations. In order to evaluate the AgTU method more thoroughly, we modified the AgTU method by adding a desorption step. In addition, we developed a new flow-through column method to measure the FES of clays assuming more effective ion-exchange can be obtained under flow-through conditions than by using batch conditions.

Our goal of this research is to estimate the effectiveness of three techniques at measuring the FES density of pristine Hanford sediments, and to further provide the most suitable method to measure the density of high-affinity Cs sorption sites on hyperalkaline-weathered Hanford sediments. These three methods are: (1) the AgTU method; (2) the modified AgTU method with a desorption step; and (3) a flow-through

exchange method. Also, since hyperalkaline-weathered Hanford sediments accumulate Cs during the weathering process, we also used Rb as a replacement of Cs in the methods as Rb is strongly competitive with Cs for sorption on FES ($\log {}^{Cs}_{K}K_c$= 4.6, and $\log {}^{Rb}_{K}K_c$ = 2.2).

3.2 Materials and Methods

3.2.1 AgTU Method Using Cs or Rb as the Sorptive

The AgTU method was modified from de Koning et al. (27). $AgNO_3$ (1.274 g) was dissolved in 150 mL of 18.2 Megaohm (MΩ) water, and thiourea (3.806 g) was dissolved in 250 mL of 18.2 MΩ water. The 0.015 M AgTU solution was prepared by slowly adding the 150 mL of $AgNO_3$ solution to the 250 mL of thiourea solution and 18.2 MΩ water was added to a total volume of 500 mL. The amount of 0.08 g air-dried pristine Hanford sediments was placed in 2-mL homo-polymer centrifuge tubes with 1.8 mL of 0.015 M AgTU solution. The samples were shaken for 24 h, centrifuged (30 min., 15,300 rcf), and the supernatant was discarded. Either 1.8 mL of $5x10^{-5}$ M $CsNO_3$ or 1.8 mL of $5x10^{-5}$ M $RbNO_3$ was added to the tubes afterwards. The samples were shaken for another 24 h and centrifuged (30 min., 15,300 rcf) again. The supernatant was then collected for analysis of Cs or Rb concentration by ICP-MS (Perkin-Elmer, Elan 9000). Cs or Rb adsorption on FES was calculated as the difference between the initial Cs (Rb) and remaining Cs (Rb) in the supernatant. We conducted the experiment with $RbNO_3$ in addition to $CsNO_3$ since the reacted sediments already contained Cs from contact with the tank waste. Rb is one of the most competitive cations with Cs to sorb

on the FES, so we hypothesize that Rb could be used to measure the FES of sediments containing appreciable Cs in the future.

3.2.2 Modified AgTU Method with a Desorption Technique

In order to address concerns with the AgTU method (15), we have applied two desorption steps following a drying step designed to enhance inner-sphere Cs sorption on the FES (Figure 3.1). In the first desorption step, Ca was used to desorb Cs from any planner and edge-hydroxyl sites not effectively blocked by the AgTU. This was followed by desorption of the FES-bound Cs using KCl as a comparison to the deductible calculation. The amount of 0.2 g air-dried pristine Hanford sediments was placed in Teflon FEP centrifuge tubes with 30 mL of 0.015 M AgTU solution. The samples were shaken for 24 h, centrifuged (20 min., 27,000 rcf), and the supernatant was discarded. Then, 30 mL of $5x10^{-5}$ M $CsNO_3$ was added to the tubes afterwards. The samples were shaken for another 24 h and centrifuged (20 min., 27,000 rcf) again. The supernatant was then collected for Cs analysis. The remaining samples were suspended in 30 mL of 95% ethanol, shaken for 1 min. and centrifuged (10 min., 27,000 rcf) to remove any entrained solution. This process was repeated three times. The sediments were then dried in the centrifuge tubes at 35°C for 24 h. After the drying step, the samples were suspended in 30 mL of 1 M $CaCl_2$ (pH 6), shaken for 30 min, and centrifuged (20 min., 27,000 rcf). This $CaCl_2$ saturation process was repeated five times and the supernatant was collected separately each time. Then, 30 mL of 1 M KCl was added into tubes. The samples were shaken for 30 min. and centrifuged (20 min., 27,000 rcf). This KCl saturation process was repeated three times and the supernatant was collected

separately in each time. Finally, the amount of Cs in each supernatant was measured by ICP-MS (Perkin-Elmer, Elan 9000). Under ideal conditions, the [FES-Cs^+] = [Cs^+ extracted by KCl] = [the initial solution Cs^+] – [the remaining solution Cs^+] – [the sorbed Cs^+ displaced by $CaCl_2$].

3.2.3 Flow-Through Technique Using Cs or Rb

The columns were prepared by packing ~1.8 g of air-dried pristine Hanford sediments into the 6.547 x 10^{-2} m I.D. X 2.1 x 10^{-2} m long (pack length) columns, yielding an average porosity of 0.52. The packed columns were subjected to continuous leaching at a uniform flow rate (~0.05 mL min^{-1}). All solutions were delivered to the columns via PTFE tubing in the following order: (a) 0.1 M $CaCl_2$ solution was delivered to the columns for 48 h corresponding to ~176 pore volumes (PVs). Effluent samples were collected approximately every 2 h within the first 12 h, and then every 9 h for the next 36 h. (b) A mixture of 0.1 M $CaCl_2$ + 10^{-4} M CsCl (or RbCl) was delivered to the columns for 72 h corresponding to ~264 PVs. During this period, effluent samples were collected every 2 h for the first 12 h, and then every 10 h for the next 60 h. (c) A 0.1 M $CaCl_2$ solution was delivered to the columns for 24 h corresponding to ~88 PVs. During this period effluent samples were collected every 2 h within the first 12 h, and then collected again after another 12 h. (d) A mixture of 0.1 M $CaCl_2$ + 0.1 M KCl was delivered to the columns for 72 h corresponding to ~264 PVs. During this period, effluent samples were collected every 2 h within the first 12 h, and then every 10 h for the next 60 h. All effluent samples were collected in parafilm-sealed PPCO tubes. The concentration of Ca and K in the effluents was analyzed by AA (Perkin-Elmer, AAnalyst 200) and the

concentration of Cs was analyzed by ICP-MS (Perkin-Elmer, Elan 9000). A Ca^{2+} concentration of 100 mmol L^{-1} was maintained throughout the leaching process to serve as a blocking agent on the planar sites, and K^+ was used in the final step to desorb the FES-bound Cs (or Rb). The [FES-Cs] was calculated as the Cs (Rb) desorption extracted by K^+.

3.3 Results and Discussion

The FES density measured with the AgTU method using Cs was 1.05 $mmol_c$ kg^{-1} (1.19% of total CEC) while it was 0.6 $mmol_c$ kg^{-1} (0.68% of total CEC) with the AgTU method using Rb (Table 3.1). The result from the modified AgTU method with the desorption steps was the lowest with only 0.10 $mmol_c$ kg^{-1} (0.11% of total CEC) (Table 3.1). This value was calculated as the Cs desorption from the K extraction on the FES. The Cs desorption from planar sites decreased with each $CaCl_2$ rinse. The Cs desorption from FES also decreased with each KCl rinse. The last (3rd) time of Cs desorption even approached to zero (Figure 3.2). Ideally, [FES-Cs^+] = [Cs^+ extracted by KCl] = [the initial sorptive Cs^+] – [the remaining sorptive Cs^+] – [the sorbed Cs^+ displaced by $CaCl_2$]. However, the calculated FES density would be negative if reported from [FES-Cs^+] = [the initial sorptive Cs^+] – [the remaining sorptive Cs^+] – [the sorbed Cs^+ displaced by $CaCl_2$]. These two methods for calculating FES density yield different results. This suggests Ca over-extracts Cs not only from the planar sites but also from other FES or exchange sites. That is why [FES-Cs^+] = [Cs^+ extracted by KCl] was significantly lower than the measurements from other methods. This is also supported

by Figure 3.2 which shows a consistency of Cs desorption by K extraction following by Ca extraction.

For the flow-through method, the FES densities measured from using Cs and Rb were very similar, 1.21 $mmol_c\ kg^{-1}$ (1.35% of total CEC) from Cs and 1.19 $mmol_c\ kg^{-1}$ (1.37% of total CEC) from Rb. These values were calculated as Cs or Rb desorption from K extraction. The desorption of cations shows that either Cs or Rb was exchanged after the introduction of KCl to the sediments (Figure 3.3 and Figure 3.4). In addition, Zachara et al. (15) used AgTU method to measure the FES density of unreacted Hanford sediment, and they obtained 0.794 $mmol_c\ kg^{-1}$, which was 1.86% of total CEC. The result in Steefel et al. (13) was 0.02 and 1.53 $mmol_c\ kg^{-1}$ for FES-1 and FES-2, yielding 1.28% of total CEC (Table 3.1). Figure 3.5 shows the comparison of the FES density in terms of percentage of total CEC from all the methods and the previous studies. Overall, the AgTU method with the use of Cs and the flow-through technique with the use of Cs and Rb gave similar FES densities (% of CEC), and the results were also consistent with the values reported in previous research (13, 15).

3.4 Literature Comparisons

Compared to the results in the literature (13, 15), the FES density (% of CEC) of pristine Hanford sediments measured from the AgTU method with Cs and the flow-through technique with Cs and Rb in this research are similar (Figure 3.5). This disagrees with the concerns of AgTU method raised by Zachara et al. (15). They proposed that AgTU might not be an effective blocking agent for planar sites at intermediate to higher Cs

concentration (e.g. Hanford sediments). However, our results (% of CEC) from the AgTU method with the use of Cs is consistent with the three-site modeling results from Steefel et al. (13) and the results from the flow-through technique with the use of Cs and Rb in this research. This suggests the AgTU complex effectively blocks the planar sites in the Hanford sediments. In the AgTU method, the FES density of pristine Hanford sediments from Rb measurement is only 60% of the Cs measurement. This suggests that FES has a higher affinity for Cs than for Rb at low concentration ($5x10^{-5}$ M) of Cs and Rb, which means Cs is a more competitive ion than Rb for replacement of K on the FES in the pristine Hanford sediments. This corresponds to the selectivity coefficients of Cs-K ($\log {}^{Cs}_{K}K_c$) and Rb-K ($\log {}^{Rb}_{K}K_c$) calculated for the FES of illite in Bradbury et al. (46). Their results show that $\log {}^{Cs}_{K}K_c$ is 4.6, and $\log {}^{Rb}_{K}K_c$ is only 2.2. However, in the flow-through method, Rb is more comparable with Cs to sorb on the FES since the higher concentration of Cs and Rb (10^{-4} M) was used. Even though FES have a higher affinity for Cs, the Rb concentrations used in this experiment were sufficient to saturate all the FES. That is why the similar FES densities of pristine Hanford sediments were obtained from the flow-through technique with the use of Cs and Rb (Figure 3.5).

3.5 Conclusions

This research tests several possible methods for directly measuring the FES density of pristine Hanford sediments. We find the commonly used AgTU method is quite effective on the Hanford site sediments. In addition, our flow-through technique appears to give reliable estimates of the FES density. At intermediate to high Cs

concentration, the use of Cs could be replaced by Rb in the method in order to measure the FES density of the Cs-containing clay minerals. Future work aims to apply the AgTU method and the flow-through technique on hyperalkaline-weathered Hanford sediments.

Table 3.1. The total CEC and FES density of pristine Hanford sediments measured from different methods and previous studies ($mmol_c\ kg^{-1}$).

	CEC	FES Site 1	FES Site 2	FES % of CEC
Zachara et al., 2002 – AgTU method	42.6	0.794		1.86
Steefel et al., 2003 – Two-site model	121.55	0.02	1.53	1.28
AgTU method (Cs desorption)	$87.9_{(9)}$	$1.05_{(1)}$		1.19
AgTU method (Rb desorption)	$87.9_{(9)}$	$0.60_{(0)}$		0.68
Modified AgTU method + Desorption technique	$87.9_{(9)}$	$0.10_{(0)}$		0.11
Flow-through technique (Cs desorption)	$87.9_{(9)}$	$1.21_{(9)}$		1.37
Flow-through technique (Rb desorption)	$87.9_{(9)}$	1.19		1.35

The subscripts are the standard deviations in concise form [e.g., $87.9_{(9)}$ = 87.9 ± 0.9 and $1.21_{(9)}$ = 1.21 ± 0.09].

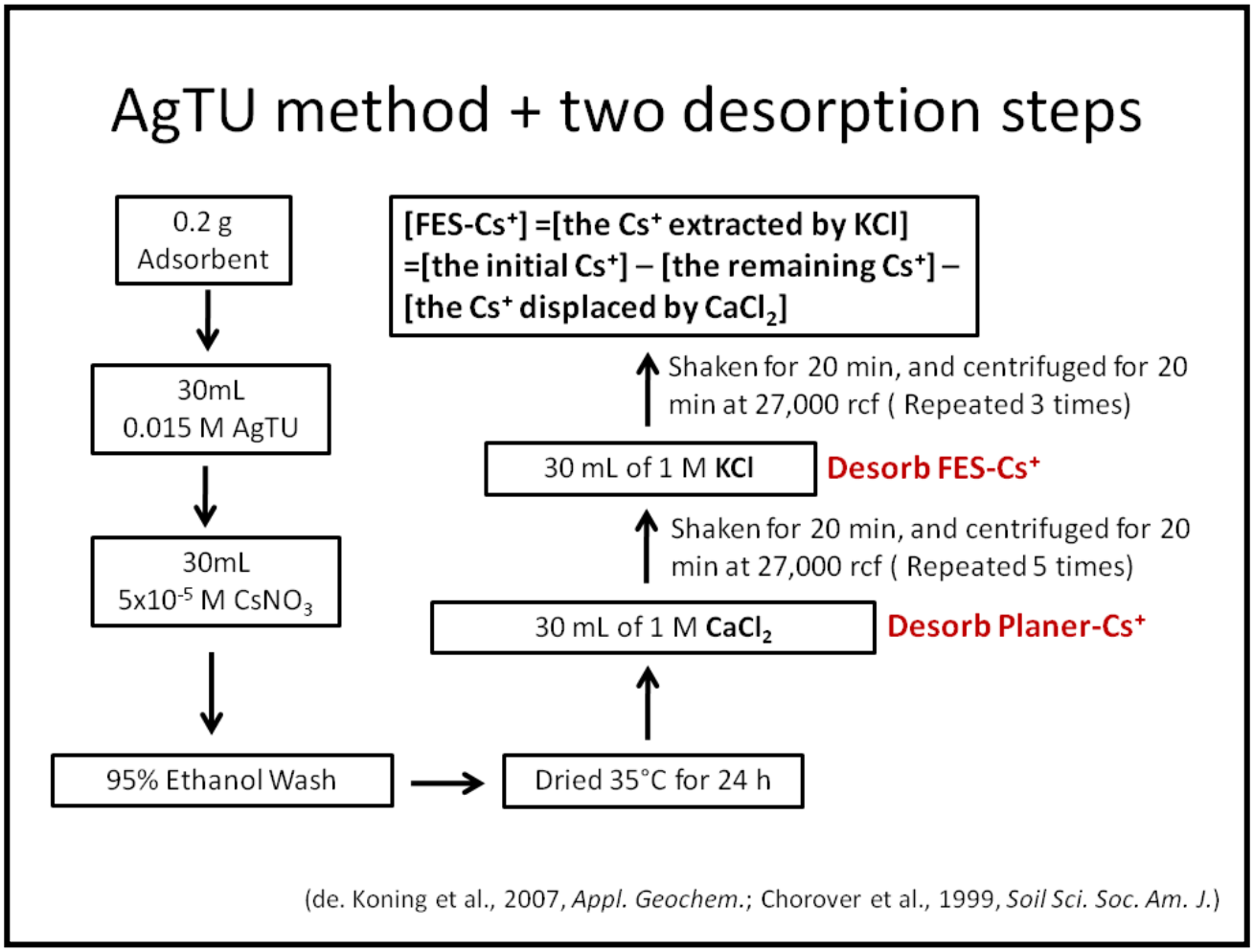

Figure 3.1. The modified AgTU method. Ca^{2+} was used to desorb the sorptive Cs on planar sites, and K^{+} was used to extract the sorptive Cs on FES.

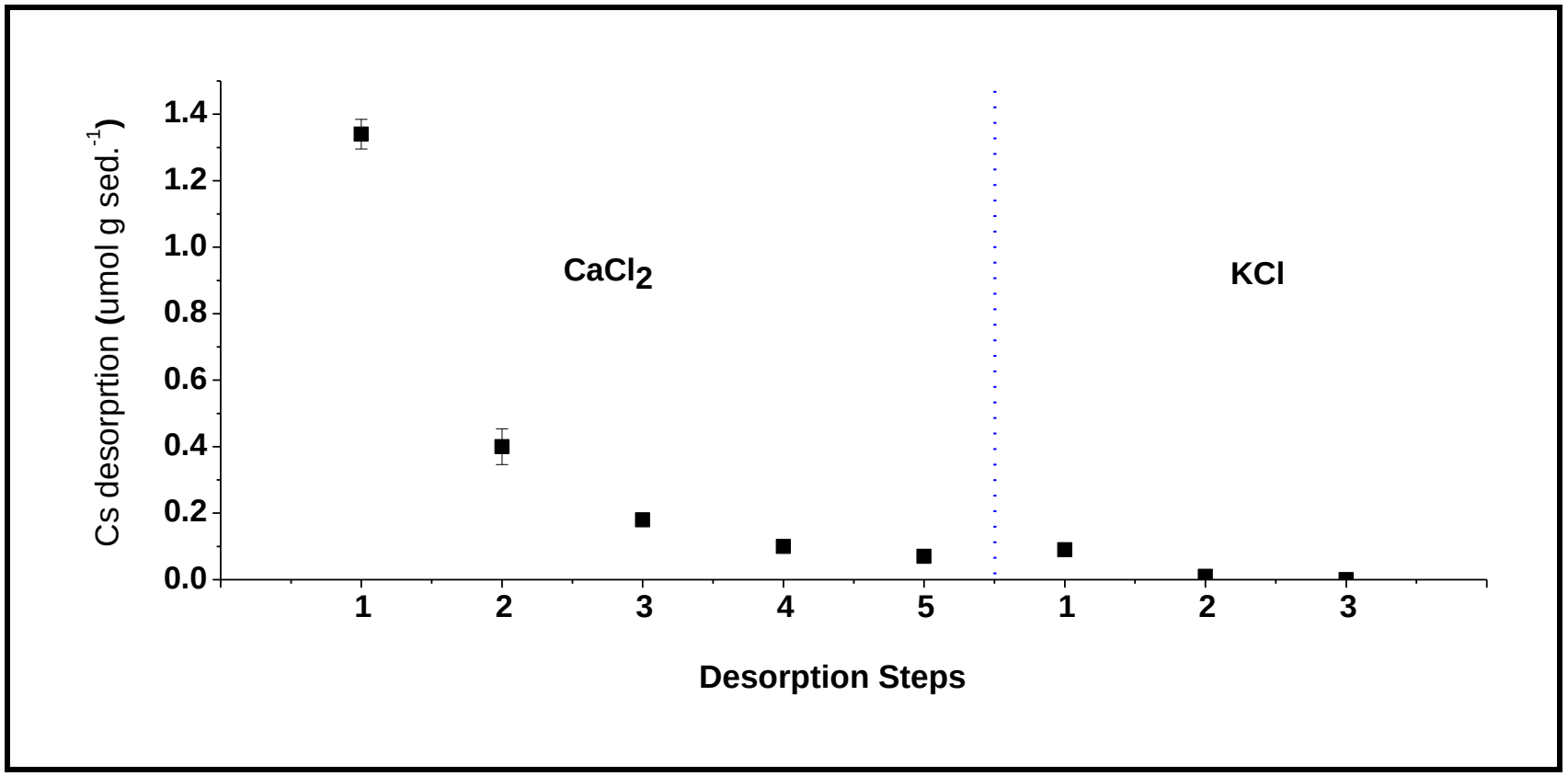

Figure 3.2. Cs desorption during various steps in the modified AgTU method.

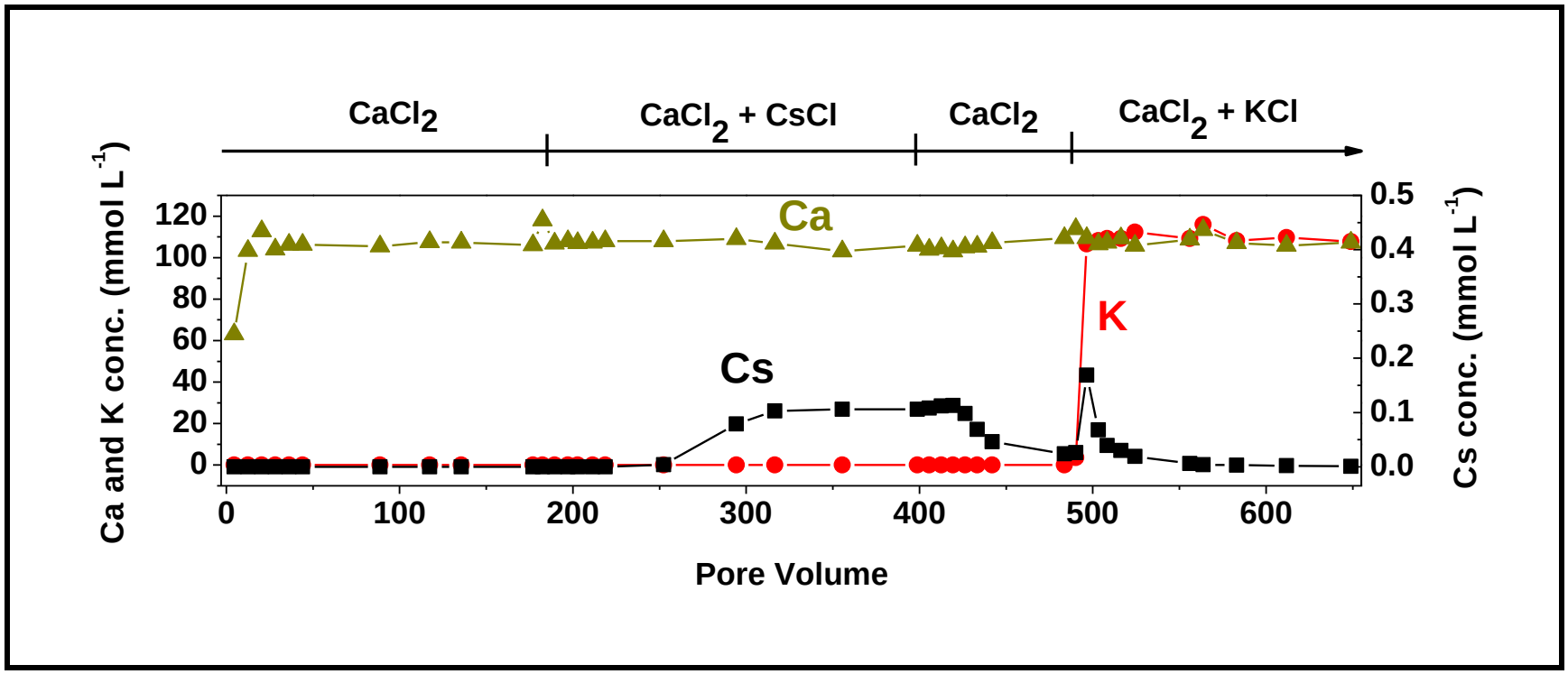

Figure 3.3. Desorption of Ca, K and Cs from pristine Hanford sediments using the AgTU method with Cs as the sorptive. The introduced influent solutions during each step are indicated above.

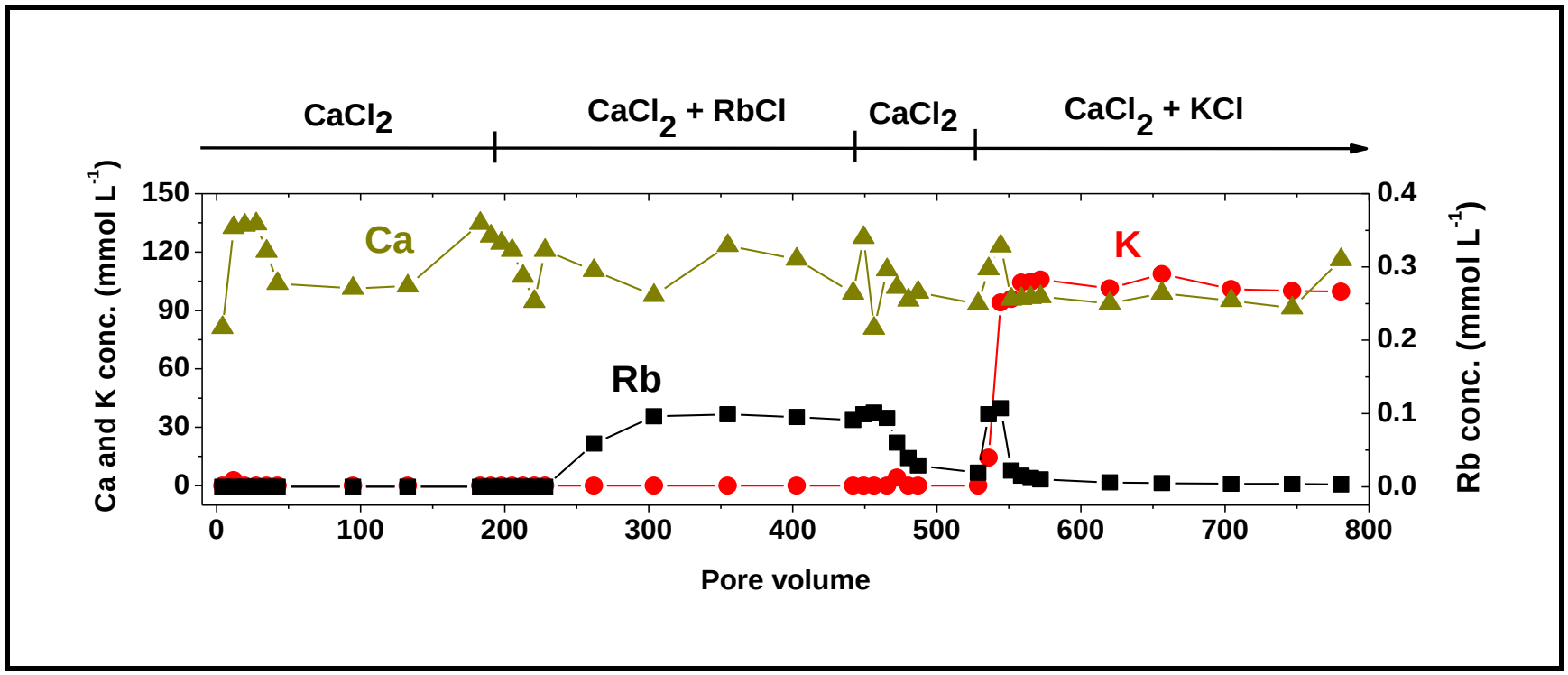

Figure 3.4. Desorption of Ca, K and Rb from pristine Hanford sediments using the AgTU method with Rb as the sorptive**.** The introduced influent solutions during each step are indicated above.

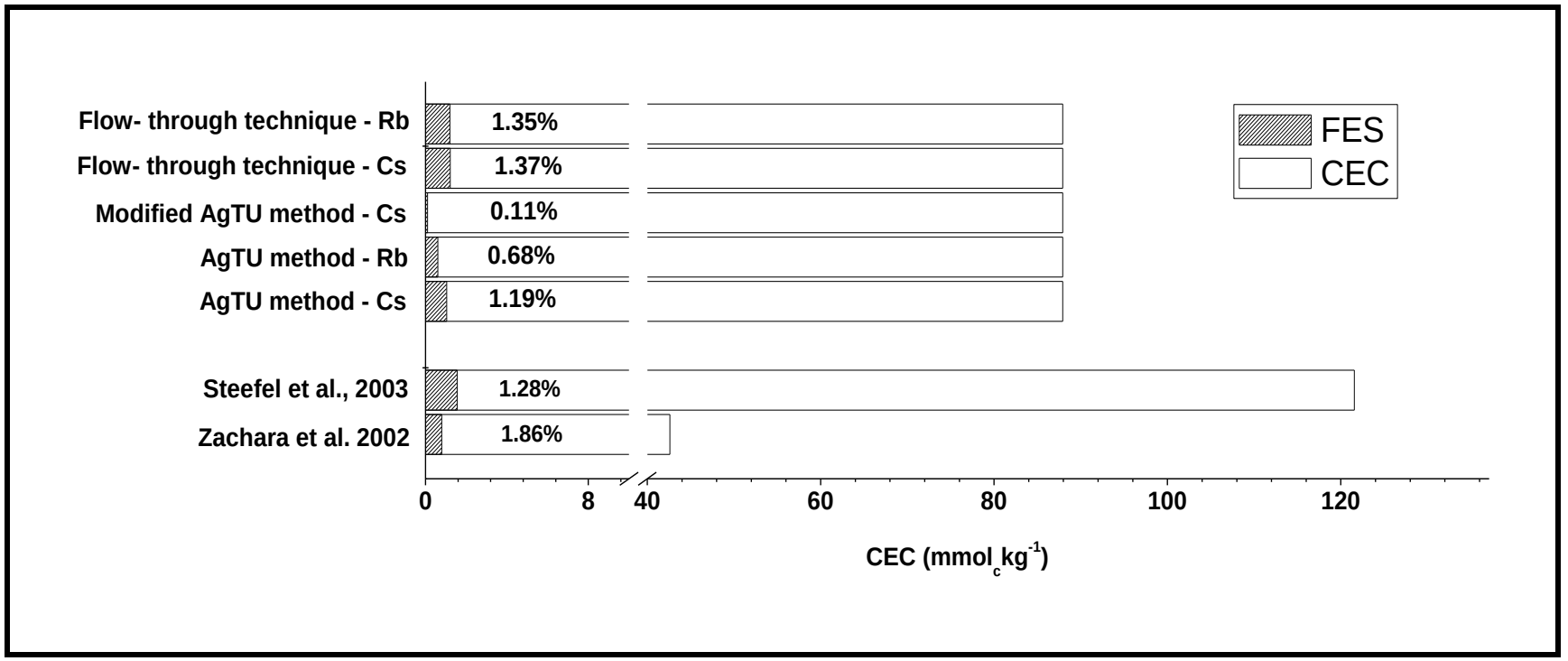

Figure 3.5. The FES density of pristine Hanford sediments in terms of the percentage of total CEC.

CHAPTER 4

ALTERATION OF HIGH-AFFINITIY CESIUM SORPTION SITES FOLLOWING HYPERALKALINE WEATHERING OF HANFORD SEDIMENTS[1]

[1] Deng, Y.T., P. A. Schroeder, A. Thompson. To be submitted to Environmental Science & Technology.

Abstract

The environmental distribution of monovalent ions with large ionic radii, such as Cs^+, K^+, Rb^+ and NH_4^+, is strongly governed by the abundance of high-affinity sorption sites on clay minerals. In most sediments, the wedge-shaped zone between non-expanded (1.0 nm) and expanded (1.4 nm) layers of micaceous clay minerals, the so called frayed-edge site (FES), is the predominate high-affinity site (HAS) for these cations. In fact, the density of FESs for a given clay is a key parameter in ion-exchange models used to predict the behavior of radioactive Cs^+ in sediments underlying the Hanford Site in Hanford, WA. Current models rely on the FES density measured for pristine Hanford sediments; however, the hyperalkaline radioactive waste is well known to drive a series of rapid mineral dissolution and precipitation reactions that likely alter the abundance of FES as well as potentially create new HAS associated with feldspathoid and zeolite neo-precipitates in these sediments. Using a suite of methods (AgTU method and Flow-through technique), we directly measured the density of HAS in pristine and hyperalkaline-weathered Hanford sediments exposed to high or low concentrations of Cs, Sr and I for 6 months or 12 months under either CO_2-free or atmospheric CO_2 conditions. We found hyperalkaline-weathering of these sediments increased the density of high affinity Cs adsorption sites relative to pristine Hanford sediments. More extensive development of HAS is found in treatments weathered under high contaminant concentration or low headspace CO_2. High contaminant concentrations favor the formation of zeolites over feldspathoids and the absence of headspace CO_2

favors the formation of stratlingite. This indicates these neo-formed minerals increase the capacity of Cs sorption.

4.1 Introduction

Zeolites and feldspathoids are two minerals that have been observed to form in the Hanford sediments with the contact of radioactive hyperalkaline wastes at DOE's Hanford Site, WA (4-6, 35, 36). These neo-formed minerals can incorporate Cs and Sr in their structural framework during their formation (6, 17, 18). Many studies have shown that Cs sorption on frayed-edge sites (FES) and other high-affinity sorption sites controls Cs transport in the subsurface environment (13-15, 21-24, 46, 47). For example, Man et al. (26) proposed two distinct environments for Cs sorption in clay minerals, including (1) outer-sphere complexes at which Cs is easily exchangeable with Na, and (2) one or more inner-sphere complexes in the ditrigonal cavity or on FES at which Cs is sorbed tightly and less exchangeable. Wampler et al. (48) also indicated that Cs and Rb may be fixed at the interlayer wedge zones within hydroxyl-interlayered vermiculite (HIV) of highly weathered coastal plain soils. Most previous work has focused on measuring or modeling the FES density of pristine Hanford sediments (13, 15). Yet, the density of FES and other high-affinity Cs sorption site is likely altered when Hanford sediments are exposed to the hyperalkaline waste solutions containing radioactive Cs. Thus, quantifying the density of FES and other high-affinity Cs sorption sites on hyperalkaline-weathered Hanford sediments is critical for accurate construction of models predicting Cs fate and transport.

It is well-known that mineral transformation can cause the alteration of FES or other high-affinity Cs sorption sites and further alter the sorption behavior of Cs in clay minerals (7, 25, 28-30, 36, 49). Mckinley et al. (30) indicated that Cs favors the area where K was depleted. This suggests that the weathering reactions cause the formation of FES within the micas. Zhao et al. (36) observed that feldspathoids (cancrinite and sodalite) sorb an order of magnitude more Cs than the unaltered kaolinite because of the high degree of Si substitution by Al, yielding structural higher charge imbalance. However, Mashal et al. (7) suggested that the mineral transformation in simulated tank waste of the Hanford site may result in a net loss of high-affinity Cs sorption sites. Therefore, future work is needed to confirm the impact of the weathering process (the formation of neo-formed minerals) on altering FES and other high-affinity Cs sorption sites in Hanford sediments.

Our goal of this research is to directly measure the density of Cs high-affinity sites (HAS) of hyperalkaline-weathered Hanford sediments using the preferred methods developed in chapter 3, including (1) AgTU methods with the use of Cs and Rb; and (2) Flow-through technique with the use of Cs and Rb. For these reacted sediments, we anticipate these Cs HAS will comprise both FES as well as other high-affinity Cs sorption sites associated with the neo-formed minerals. By comparing the results of each treatment (6 month/12 month, high/low contaminant concentration, and [+CO_2]/[-CO_2]) with pristine Hanford sediments, the impact of weathering process on Cs HAS (the FES and other high-affinity Cs sorption sites) can be assessed.

4.2 Materials and Methods

4.2.1 AgTU Method Using Cs or Rb as the Sorptive

As described in chapter 3, we added 0.08 g air-dried reacted Hanford sediments (sediment contamination as illustrated in chapter 2 or Appendix B) to 2-mL homo-polymer centrifuge tubes with 1.8 mL of 0.015 M AgTU solution. The samples were shaken for 24 h, centrifuged (30 min., 15,300 rcf), and the supernatant was discarded. Either 5 mL of $5x10^{-5}$ M $CsNO_3$ or 5 mL of $5x10^{-5}$ M $RbNO_3$ was added to the tubes afterwards. The samples were shaken for another 24 h and centrifuged (30 min., 15,300 rcf) again. The supernatant was then collected for analysis of Cs or Rb concentration by ICP-MS (Perkin-Elmer, Elan 9000). Cs or Rb adsorption on Cs HAS was calculated as the difference between the initial Cs (Rb) and remaining Cs (Rb) in the supernatant. The FES of Hanford unreacted sediment was also evaluated in this experiment as an experimental control.

4.2.2 Flow-Through Technique Using Rb as the Sorptive

The columns were prepared by packing ~1.8 g of reacted Hanford sediments into the 6.547×10^{-2} m I.D. X 2.1×10^{-2} m long (pack length) columns, yielding an average porosity of 0.52. The packed columns were subjected to continuous leaching at a uniform flow rate (~0.05 mL min^{-1}). All solutions were delivered to the columns via PTFE tubing in the following order. The influent solutions: (a) 0.1 M $CaCl_2$ solution was delivered to the columns for 48 hr corresponding to ~176 pore volumes (PVs). The effluent samples were collected approximately every 2 h within the first 12 h, and then approximately every 9 h for the remaining 36 h. (b) The mixture of 0.1 M $CaCl_2$ + 10^{-4} M

RbCl was delivered to the columns for 72 h corresponding to ~264 PVs. The effluent samples were collected approximately every 2 hr within the first 12 h, and then approximately every 10 h for the remaining 60 h. (c) 0.1 M $CaCl_2$ solution was delivered to the columns for 24 h corresponding to ~88 PVs. The effluent samples were collected approximately every 2 h within the first 12 h, and then collected again after another 12 h. (d) The mixture of 0.1 M $CaCl_2$ + 0.1 M KCl was delivered to the columns for 72 h corresponding to ~264 PVs. The effluent samples were collected approximately every 2 h within the first 12 h, and then approximately every 10 h for the remaining 60 h. The effluent samples were collected in parafilm-sealed PPCO tubes. The concentration of Ca and K in the effluent samples was analyzed by AA (Perkin-Elmer, AAnalyst 200) and the concentration of Rb was analyzed by ICP-MS (Perkin-Elmer, Elan 9000). Ca^{2+} through the whole leaching was served as the blocking agent for planar sites, and K^+ in the final step was used to desorb the HAS-bound Rb, which was calculated as the Rb desorption extracted by K^+.

4.3 Results

4.3.1 HAS Density from AgTU Method Using Cs or Rb as the Sorptive

The HAS density of pristine Hanford sediments calculated from sorption of Rb was ~60% of that calculated from Cs sorption (Table 4.1). This can be attributed to Rb's lower affinity to FES as illustrated in chapter 3. The HAS density (expressed as a percentage of sediment CEC) of most treatments calculated from Rb and Cs as the sorptive were two times higher than FES density of pristine Hanford sediments except

the LOW treatment C3: 12 month L+C and C4: 6 month L+C (Table 4.1). Regardless of which ion was used to probe the surface sites, when sediments were weathered in the presence of headspace CO_2 [$+CO_2$], those with high contaminant concentrations (HIGH) exhibited a greater increase in Cs (or Rb) HAS than those with low contaminant concentrations (LOW). In contrast, no change in the density of HAS was detected between HIGH and LOW treatments in the absence of pCO_2 [$-CO_2$] (Figure 4.1).

4.3.2 HAS Density from Flow-Through Technique Using Rb as the Sorptive

The density of HAS (% of CEC) for the pristine Hanford sediments calculated using our flow-through sorption method with Rb as the sorptive/sorbate was similar to the measurements from the AgTU method using Cs as the sorptive. However, the HAS density of all the reacted sediments calculated using the flow-through technique with Rb as the sorptive was significantly higher than the HAS density calculated from the AgTU method with Cs as the sorptive (Figure 4.1). Among all the treatments, the HAS density of the [$-CO_2$] treatments was higher than that of the [$+CO_2$] treatments and uniformly the HIGH treatments exhibited greater HAS density than the LOW treatments (Table 4.2 and Figure 4.1). Examination of the cation release curves following the addition of KCl reveals that during leaching Rb was displaced from the sorption sites in all treatments and in the HIGH treatments Cs was also displaced (Figure 4.2 and Figure 4.3). This suggests that K also displaced some contaminant Cs from the exchangeable sites that was not effectively displaced by Rb in the earlier Rb sorption step (Figure 4.3).

4.4. Discussion

4.4.1 Influence of Neo-mineral Formation on HAS Density

Despite a consistent decrease in the CEC of the hyperalkaline-weathered sediments (Appendix A), the density of HAS increased for all reacted treatments. Our data suggests that weathering reactions generate more HAS for Cs and Rb sorption. More specifically, the mineral formation of illite, feldspathoid, and zeolite in the reacted sediments alters the behavior of Cs sorption (7).This is consistent with Zhao et al. (36) but contrary to the result in Mashal et al. (7). Zhao et al. (36) proposed that feldspathoids sorb more Cs than the unaltered Kaolinite while Mashal et al. (7) suggested that the mineral transformation of Hanford sediments may result in a net loss of high-affinity Cs sorption sites.

Also, the HAS density is the greatest for the sediments weathered under HIGH contaminant concentration suggesting that neo-formed mineral “zeolite”, which formed preferentially in the HIGH treatments, provides more HAS to Cs and Rb than the NO_3-feldspthoisds, which formed preferentially in the low treatments (Table 4.3). This is consistent with zeolite’s high cation exchange capacity (50-52). Feldspathoid also has high CEC, however it is possible that Rb is incorporated in the framework of feldspathoid during the sorption step of our experiment and becomes more resistant to exchange with K than when sorbed in the zeolite phases (16), which may result in lower measurements of HAS. In addition, according to Table 4.3 from Perdrial et al. (6), illite formation increases in the HIGH treatments during the weathering reactions (6), and it is known that micaceous materials (illite in this case) have a high capacity for Cs sorption

(7, 28, 46). It also appears that the lower partial pressure of CO_2 ([-CO_2] treatments) during the weathering process increases the development of HAS. This could be the contribution of the neo-formed mineral "stratlingites [$Ca_2Al_2SiO_7 \cdot 8(H_2O)$]", which preferentially formed in the [-CO_2] treatments (Table 4.3). Although no studies have discussed the CEC of stratlingites, Shrivastava et al. (53) indicated substituted tobermorites [$(Ca_5Si_6O_{16} \cdot (OH)_2 \cdot 4(H_2O)$] with different level of [Al+Na] have high CEC and very high selectivities for Cs^+. Thus, we hypothesize that Stratlingites, which form when $CaCO_3$ dissolution reacts with Al from Hanford wastes and Si from silicate mineral dissolution (6), would have higher selectivity to Cs.

4.5. Conclusions

The capacity of Cs or Rb sorption increases in the reacted sediments compared to pristine Hanford sediments, which indicates that the weathering process increases the HAS. Among all the treatments, the HIGH and [-CO_2] treatments have the greatest HAS density, which is contributed from the formation of illite, zeolite, and stantlingite. Future work should focus on using different microscopy techniques to visually assess the contribution of the neo-formed minerals to alter Cs HAS, and to further distinguish the FES and other high-affinity Cs sorption sites of hyperalkaline-weathered Hanford sediments.

Table 4.1. The HAS density ($mmol_c\ kg^{-1}$) of hyperalkaline-weathered Hanford sediments from the AgTU method using Cs and Rb as the sorptive.

	Treatments	Rb	%FES	Cs	%FES
HF	Unreacted	$0.60_{(0)}$	0.68	$1.05_{(1)}$	1.19
C1	6mon H+C	$0.75_{(0)}$	1.29	$1.21_{(1)}$	2.08
C2	12mon H+C	$0.76_{(0)}$	1.36	$1.23_{(0)}$	2.18
C3	12mon L+C	$0.67_{(0)}$	1.02	$1.08_{(1)}$	1.64
C4	6mon L+C	$0.69_{(0)}$	0.91	$1.11_{(0)}$	1.48
C5	12mon H-C	$0.77_{(0)}$	1.39	$1.23_{(1)}$	2.22
C6	6mon H-C	$0.76_{(0)}$	1.41	$1.21_{(0)}$	2.26
C7	12mon L-C	$0.73_{(1)}$	1.42	$1.17_{(2)}$	2.29
C8	6mon L-C	$0.72_{(0)}$	1.21	$1.14_{(2)}$	1.92

The subscripts are the standard deviations in concise form [e.g., $0.73_{(1)} = 0.73 \pm 0.01$ and $1.17_{(2)} = 1.17 \pm 0.02$].

Table 4.2. The HAS density ($mmol_c\ kg^{-1}$) of hyperalkaline-weathered Hanford sediments from the flow-through technique using Rb as the sorptive. The Rb desorption and Cs desorption are the extraction from K^+.

	Treatments	Rb	%FES	Cs	%FES
HF	Unreacted	1.19	1.35	0.00	0.00
C1	6mon H+C	5.61	9.64	2.91	5.01
C2	12mon H+C	5.73	10.20	2.16	3.84
C3	12mon L+C	5.07	7.69	0.00	0.01
C4	6mon L+C	5.18	6.90	0.01	0.01
C5	12mon H-C	7.94	14.39	4.28	7.77
C6	6mon H-C	6.58	12.26	4.21	7.83
C7	12mon L-C	4.70	9.23	0.00	0.01
C8	6mon L-C	4.81	8.10	0.01	0.01

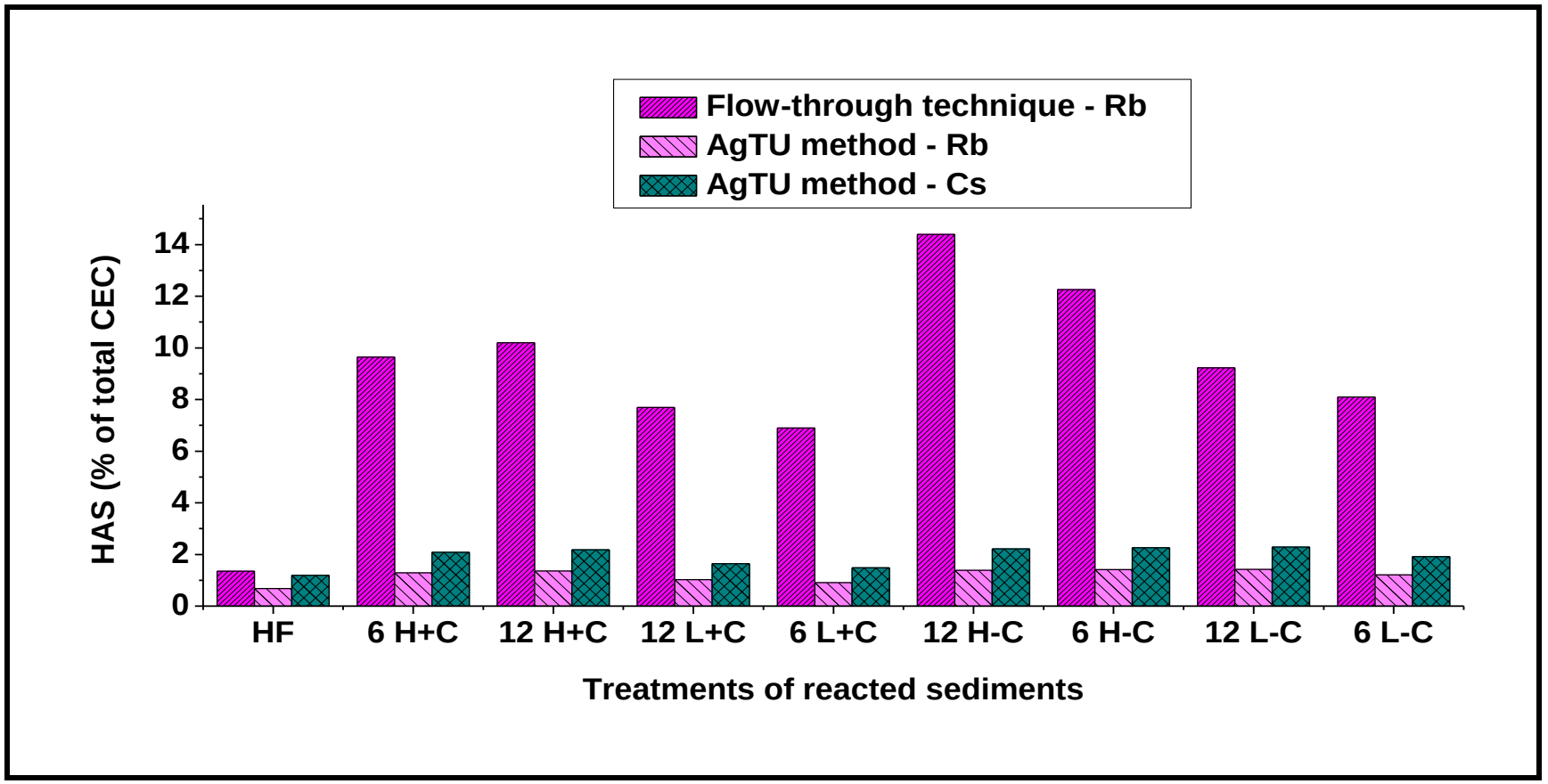

Figure 4.1. The HAS density (% of total CEC) comparison of hyperalkaline-weathered Hanford sediments calculated from different methods.

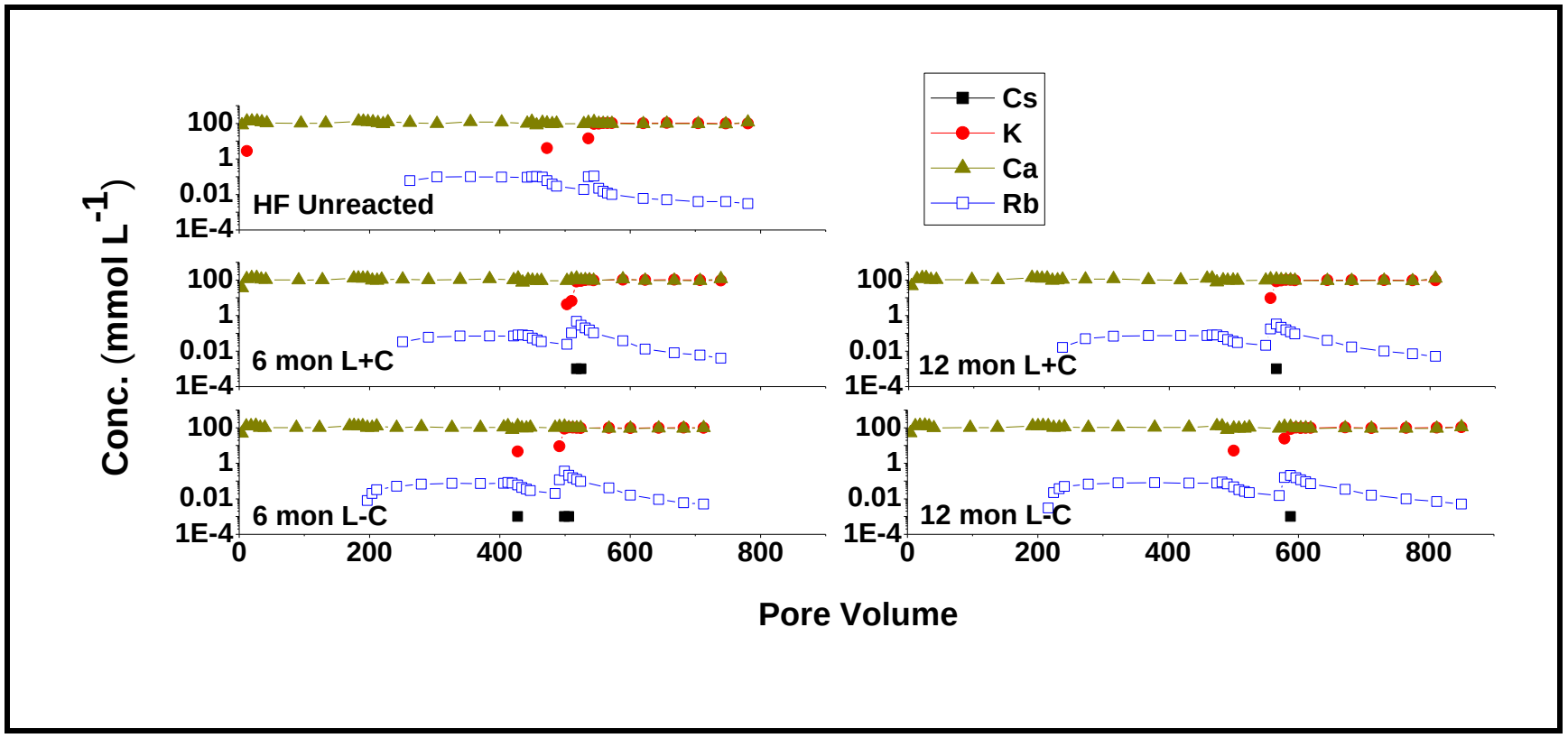

Figure 4.2. Desorption of Ca, K, Rb, and Cs from the LOW using the flow-through technique with Rb as the sorptive.

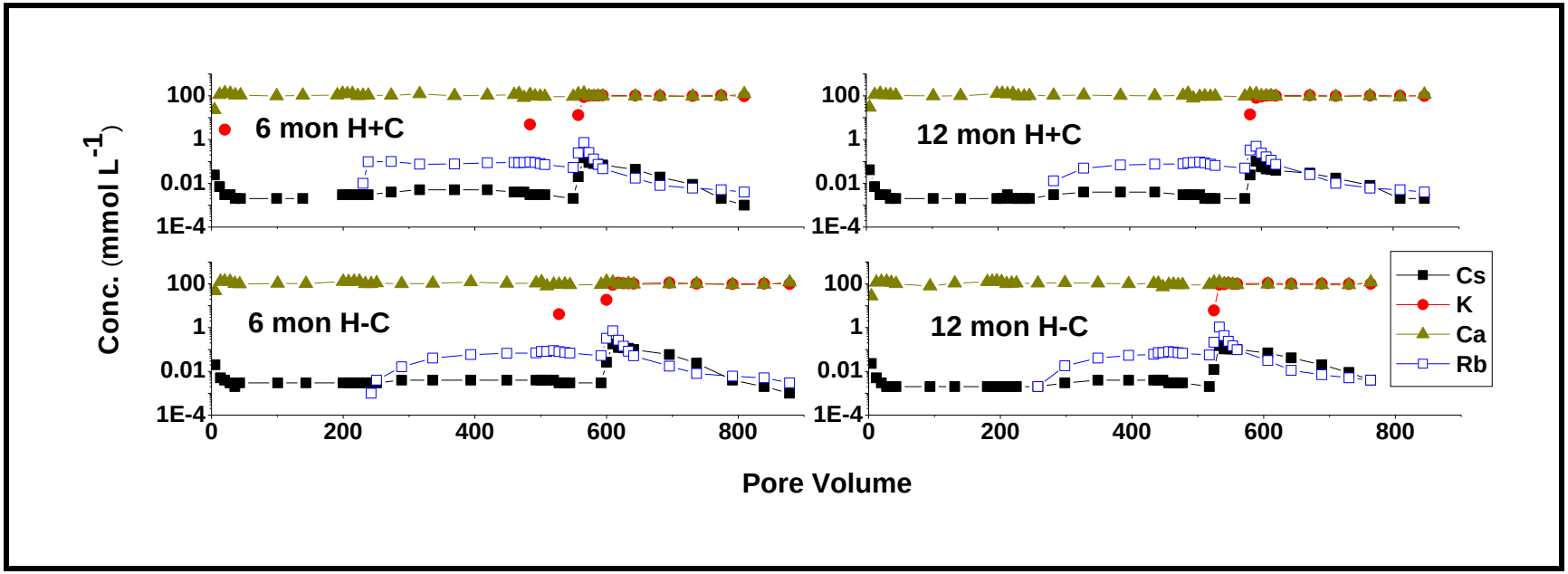

Figure 4.3. Desorption of Ca, K, Rb, and Cs from the HIGH treatments using the flow-through technique with Rb as the sorptive.

Table 4.3. Quantitative results (in %) of the Rietveld simulation performed on the unreacted and reacted fine fraction extracts (6).

Sample name	Quartz SiO_2	Albite $NaAlSi_3O_8$	Andesine $(Ca,Na)(Al,Si)_4O_8$	Illite $K(Al,Mg,Fe)_2(Si,Al)_4O_{10}[(OH)_2 \cdot (H_2O)]$	Chlorite $(Fe,Mg,Al)_6(Si,Al)_4O_{10}(OH)_8$	Kaolinite $Al_2Si_2O_5(OH)_4$	Calcite $CaCO_3$	Sr,Ca chabazite $Ca_{1.4}Sr_{0.3}Al_{3.8}Si_{8.3}O_{24} \cdot 13H_2O$	NO_3-sodalite $Na_8(AlSiO_4)_6(NO_3)_2$	NO_3-cancrinite $Na_{7.6}(AlSiO_4)_6(NO_3)_{1.6}(H_2O)_2$	Strätlingite $Ca_2Al_2SiO_7 \cdot 8(H_2O)$	$\chi^{2\,a}$
Hanford	26.8	11.6	18.1	24.6	14.8	1.0	3.1	0.0	0.0	0.0	0.0	3.8
6mo High $+CO_2$	15.8	11.9	7.9	47.2	0.0	1.5	1.4	14.2	0.0	0.0	0.0	11.8
6mo High $-CO_2$	14.3	6.8	14.8	28.1	0.5	0.0	0.0	20.0	0.0	0.0	15.5	13.3
6mo Low $+CO_2$	24.8	4.0	18.7	20.2	8.0	2.3	7.3	0.2	10.6	4.0	0.0	15.4
6mo Low $-CO_2$	20.5	10.6	6.6	22.1	3.7	2.1	0.0	4.0	11.1	11.2	8.3	8.7
12mo High $+CO_2$	14.5	5.5	12.5	37.8	1.1	0.0	2.2	13.9	8.8	3.7	0.0	12.4
12mo High $-CO_2$	13.4	6.2	5.6	30.0	0.9	1.0	0.0	27.9	0.2	0.4	14.4	5.1
12mo Low $+CO_2$	17.7	5.9	6.2	27.5	1.1	2.1	6.4	0.1	23.6	9.3	0.0	8.3
12mo Low $-CO_2$	20.2	6.6	4.6	17.1	1.6	0.7	0.0	1.3	29.0	16.1	2.8	7.4

[a] χ^2 represents the goodness of fit and correspond to $\chi^2 = [\Sigma_i (I_{obs} - I_{calc})_i^2 / \sigma^2(I_{obs})_i] / (n - p)]$; with I the intensity, $\sigma(I_{obs})$ the estimated error of the measure (fixed to 10% of the counts), n the number of points used for simulation and p the number of parameters estimated.

CHAPTER 5

CONCLUSIONS

Our research set up three goals in order to understand the mechanism of contaminant desorption from the neo-formed minerals in hyperalkaline-weathered Hanford sediments and the impact of the weathering process on altering FES and other high-affinity Cs sorption sites. Our work has suggested that $CsNO_{3(aq)}$ and $Sr(NO_3)_{2(aq)}$ are first released as ion-pairs from the NO_3-feldspthoids which formed in the LOW treatments until the ratio of remaining NO_3 to remaining NO_3-feldspathoids reaches ~ 0.025. After that, NO_3 and the incorporated Cs and Sr are released mainly via NO_3-feldspathoid dissolution. However, the reactive-transport modeling suggests that FES-bound Cs desorption is decoupled from NO_3 desorption. Also, the results have shown that Cs release from the HIGH treatments cannot be explained solely by an ion-exchange model, which indicates that Cs release from the HIGH treatments involves the major mineral dissolution. Additionally, we discovered the AgTU method and the flow-through technique are two efficient ways to measure the FES density of sediments. Our measurements from different methods show that the FES density of pristine Hanford sediments ranges from 1.18 - 1.37% of total CEC, which is consistent with the values reported in the previous studies. However, the HAS density of hyperalkaline-weathered Hanford sediments is found to be higher than that of unreacted sediments, and the HIGH treatments with [$-CO_2$] have the greatest HAS density among all the treatments.

This suggests that the weathering process (the formation of NO_3-feldspathoids, zeolites, and stratlingites) increases the HAS.

According to our findings, the mechanism of contaminant release in the field environment depends on the mineral composition. Also, the weathering process can increase the available HAS of clay minerals and further increase Cs retention. Future work should aim to modify the existing reactive-transport models with all the experimental data to better address the Cs desorption from the HIGH treatments. Also, work of microscopy on Cs-sorbed sediments should be improved to enable the visual assessment of FES or other high-affinity Cs sorption sites. This might help further distinguish different FES which sorbs Cs to different extent as some study would propose two FES in the modeling work. Once we have better understanding of Cs transport in the environment, we can then propose a mature strategy for remediation.

REFERENCES

(1) Babad, H.; Cash, R. J.; Deichman, J. L.; Johnson, G. D. High-priority Hanford Site radioactive-waste storage tank safety issues - an overview. *J. Hazard. Mater.* **1993,** *35*, 427-441.

(2) Gephart, R. E., *Hanford: A conversation about nuclear waste and cleanup*. Battelle Press: Columbus, Ohio, 2003; p 1 v. (various pagings).

(3) Zachara, J. M.; Serne, J.; Freshley, M.; Mann, F.; Anderson, F.; Wood, M.; Jones, T.; Myers, D. Geochemical processes controlling migration of tank wastes in Hanford's vadose zone. *Vadose Zone J.* **2007,** *6*, 985-1003.

(4) Deng, Y.; Harsh, J. B.; Flury, M.; Young, J. S.; Boyle, J. S. Mineral formation during simulated leaks of Hanford waste tanks. *Appl. Geochem.* **2006,** *21*, 1392-1409.

(5) Deng, Y. J.; Flury, M.; Harsh, J. B.; Felmy, A. R.; Qafoku, O. Cancrinite and sodalite formation in the presence of cesium, potassium, magnesium, calcium and strontium in Hanford tank waste simulants. *Appl. Geochem.* **2006,** *21*, 2049-2063.

(6) Perdrial, N.; Rivera, N.; Thompson, A.; O'Day, P. A.; Chorover, J. Trace contaminant concentration affects mineral transformation and pollutant fate in hydroxide-weathered Hanford sediments. *J. Hazard. Mater.* **2011,** *197*, 119-127.

(7) Mashal, K. Y.; Cetiner, Z. S. Experimental investigation of cesium mobility in the course of secondary mineral formations in Hanford sediment columns at 50 degrees C. *Environ. Monit. Assess.* **2009,** *169*, 249-258.

(8) Hu, Q.; Zhao, P.; Moran, J. E.; Seaman, J. C. Sorption and transport of iodine species in sediments from the Savannah River and Hanford Sites. *J. Contam. Hydrol.* **2005,** *78*, 185-205.

(9) McKinley, J. P.; Zachara, J. M.; Smith, S. C.; Liu, C. Cation exchange reactions controlling desorption of Sr-90(2+) from coarse-grained contaminated sediments at the Hanford site, Washington. *Geochim. Cosmochim. Acta* **2007,** *71*, 305-325.

(10) Um, W.; Serne, R. J. Sorption and transport behavior of radionuclides in the proposed low-level radioactive waste disposal facility at the Hanford site, Washington. *Radiochimica Acta* **2005,** *93*, 57-63.

(11) Murray, C. J.; Ward, A. L.; Wilson, J. L. Influence of clastic dikes on vertical migration of contaminants at the Hanford site. *Vadose Zone J.* **2007,** *6*, 959-970.

(12) Liu, C. X.; Zachara, J. M.; Smith, S. C. A cation exchange model to describe Cs+ sorption at high ionic strength in subsurface sediments at Hanford site, USA. *J. Contam. Hydrol.* **2004,** *68*, 217-238.

(13) Steefel, C. I.; Carroll, S.; Zhao, P.; Roberts, S. Cesium migration in Hanford sediment: a multisite cation exchange model based on laboratory transport experiments. *J. Contam. Hydrol.* **2003,** *67*, 219-246.

(14) Thompson, A.; Steefel, C. I.; Perdrial, N.; Chorover, J. Contaminant desorption during long-term leaching of hydroxide-weathered Hanford sediments. *Environ. Sci. Technol.* **2010,** *44*, 1992-1997.

(15) Zachara, J. M.; Smith, S. C.; Liu, C.; McKinley, J. P.; Serne, R. J.; Gassman, P. L. Sorption of Cs^+ to micaceous subsurface sediments from the Hanford site, USA. *Geochim. Cosmochim. Acta* **2002,** *66*, 193-211.

(16) Mon, J.; Deng, Y. J.; Flury, M.; Harsh, J. B. Cesium incorporation and diffusion in cancrinite, sodalite, zeolite, and allophane. *Microporous Mesoporous Mater.* **2005,** *86*, 277-286.

(17) Rivera, N.; Choi, S.; Strepka, C.; Mueller, K.; Perdrial, N.; Chorover, J.; O'Day, P. A. Cesium and strontium incorporation into zeolite-type phases during homogeneous nucleation from caustic solutions. *Am. Mineral.* **2011,** *96*, 1809-1820.

(18) Chorover, J.; Choi, S. K.; Amistadi, M. K.; Karthikeyan, K. G.; Crosson, G.; Mueller, K. T. Linking cesium and strontium uptake to kaolinite weathering in simulated tank waste leachate. *Environ. Sci. Technol.* **2003,** *37*, 2200-2208.

(19) Chorover, J.; Choi, S.; Rotenberg, P.; Serne, R. J.; Rivera, N.; Strepka, C.; Thompson, A.; Mueller, K. T.; O'Day, P. A. Silicon control of strontium and cesium partitioning in hydroxide-weathered sediments. *Geochim. Cosmochim. Acta* **2008,** *72*, 2024-2047.

(20) Chang, H. S.; Um, W.; Rod, K.; Serne, R. J.; Thompson, A.; Perdrial, N.; Steefel, C. I.; Chorover, J. Strontium and cesium release mechanisms during unsaturated

flow through waste-weathered Hanford sediments. *Environ. Sci. Technol.* **2011,** *45*, 8313-8320.

(21) Gobran, G. R.; Wenzel, W. W.; Lombi, E., *Trace elements in the rhizosphere*. CRC Press: London, 2000; p 67-73.

(22) Poinssot, C.; Baeyens, B.; Bradbury, M. H. Experimental and modelling studies of caesium sorption on illite. *Geochim. Cosmochim. Acta* **1999,** *63*, 3217-3227.

(23) Turner, N. B.; Ryan, J. N.; Saiers, J. E. Effect of desorption kinetics on colloid-facilitated transport of contaminants: Cesium, strontium, and illite colloids. *Water Resour. Res.* **2006,** *42*, 17.

(24) Sawhney, B. L. Selective sorption and fixation of cations by clay-minerals: a review. *Clays Clay Miner.* **1972,** *20*, 93-100.

(25) Nakao, A.; Thiry, Y.; Funakawa, S.; Kosaki, T. Characterization of the frayed edge site of micaceous minerals in soil clays influenced by different pedogenetic conditions in Japan and northern Thailand. *Soil Sci. Plant Nutr.* **2008,** *54*, 479-489.

(26) Man, C. K.; Chu, P. Y. Experimental and modeling studies of radiocesium retention in soils. *J. Radioanal. Nucl. Chem.* **2004,** *262*, 339-344.

(27) de Koning, A.; Konoplev, A. V.; Comans, R. N. J. Measuring the specific caesium sorption capacity of soils, sediments and clay minerals. *Appl. Geochem.* **2007,** *22*, 219-229.

(28) Nakao, A.; Funakawa, S.; Watanabe, T.; Kosaki, T. Pedogenic alterations of illitic minerals represented by Radiocaesium Interception Potential in soils with different soil moisture regimes in humid Asia. *Eur. J. Soil Sci.* **2009,** *60*, 139-152.

(29) Maes, E.; Vielvoye, L.; Stone, W.; Delvaux, B. Fixation of radiocaesium traces in a weathering sequence mica -> vermiculite -> hydroxy interlayered vermiculite. *Eur. J. Soil Sci.* **1999,** *50*, 107-115.

(30) McKinley, J. P.; Zachara, J. M.; Heald, S. M.; Dohnalkova, A.; Newville, M. G.; Sutton, S. R. Microscale distribution of cesium sorbed to biotite and muscovite. *Environ. Sci. Technol.* **2004,** *38*, 1017-1023.

(31) Ainsworth, C. C.; Zachara, J. M.; Wagnon, K.; McKinley, S.; Liu, C.; Smith, S. C.; Schaef, H. T.; Gassman, P. L. Impact of highly basic solutions on sorption of Cs^+ to subsurface sediments from the Hanford site, USA. *Geochim. Cosmochim. Acta* **2005,** *69*, 4787-4800.

(32) Fredrickson, J. K.; Zachara, J. M.; Balkwill, D. L.; Kennedy, D.; Li, S.-m. W.; Kostandarithes, H. M.; Daly, M. J.; Romine, M. F.; Brockman, F. J. Geomicrobiology of high-level nuclear waste-contaminated vadose sediments at the Hanford Site, Washington State. *Vadose Zone J.* **2004,** *70*, 4230-4241.

(33) Gee, G. W.; Oostrom, M.; Freshley, M. D.; Rockhold, M. L.; Zachara, J. M. Hanford Site vadose zone studies: An overview. *Vadose Zone J.* **2007,** *6*, 899-905.

(34) Khaleel, R.; White, M. D.; Oostrom, M.; Wood, M. I.; Mann, F. M.; Kristofzski, J. G. Impact assessment of existing vadose zone contamination at the Hanford Site SX tank farm. *Vadose Zone J.* **2007,** *6*, 935-945.

(35) Mashal, K.; Harsh, J. B.; Flury, M. Clay mineralogical transformations over time in Hanford sediments reacted with simulated tank waste. *Soil Sci. Soc. Am. J.* **2005,** *69*, 531-538.

(36) Zhao, H. T.; Deng, Y. J.; Harsh, J. B.; Flury, M.; Boyle, J. S. Alteration of kaolinite to cancrinite and sodalite by simulated hanford tank waste and its impact on cesium retention. *Clays Clay Miner.* **2004,** *52*, 1-13.

(37) Lichtner, P. C.; Yabusaki, S.; Pruess, K.; Steefel, C. I. Role of competitive cation exchange on chromatographic displacement of cesium in the vadose zone beneath the Hanford S/SX Tank Farm. *Vadose Zone J.* **2004,** *3*, 203-219.

(38) Liu, C. X.; Zachara, J. M.; Qafoku, O.; Smith, S. C. Effect of temperature on Cs^+ sorption and desorption in subsurface sediments at the Hanford Site, USA. *Environ. Sci. Technol.* **2003,** *37*, 2640-2645.

(39) McKinley, J. P.; Zeissler, C. J.; Zachara, J. M.; Serne, R. J.; Lindstrom, R. M.; Schaef, H. T.; Orr, R. D. Distribution and retention of Cs-137 in sediments at the Hanford Site, Washington. *Environ. Sci. Technol.* **2001,** *35*, 3433-3441.

(40) Riley, R. G.; Zachara, J. M. *Chemical contaminants on DOE lands and selection of contaminant mixtures for subsurface science research*; U.S. Department of Energy, Office of Energy Research: Washington, D.C., 1992.

(41) Choi, S.; Amistadi, M. K.; Chorover, J. Clay mineral weathering and contaminant dynamics in a caustic aqueous system - I. Wet chemistry and aging effects. *Geochim. Cosmochim. Acta* **2005,** *69*, 4425-4436.

(42) Choi, S.; Crosson, G.; Mueller, K. T.; Seraphin, S.; Chorover, J. Clay mineral weathering and contaminant dynamics in a caustic aqueous system - II. Mineral transformation and microscale partitioning. *Geochim. Cosmochim. Acta* **2005,** *69*, 4437-4451.

(43) Choi, S.; O'Day, P. A.; Rivera, N. A.; Mueller, K. T.; Vairavamurthy, M. A.; Seraphin, S.; Chorover, J. Strontium speciation during reaction of kaolinite with simulated tank-waste leachate: Bulk and microfocused EXAFS analysis. *Environ. Sci. Technol.* **2006,** *40*, 2608-2614.

(44) Dontsova, K.; Steefel, C. I.; Desilets, S.; Thompson, A.; Chorover, J. Solid phase evolution in the Biosphere 2 hillslope experiment as predicted by modeling of hydrologic and geochemical fluxes. *Hydrol. Earth Syst. Sci.* **2009,** *13*, 2273-2286.

(45) Buhl, J.-C.; Stief, F.; Fechtelkord, M.; Gesing, T. M.; Taphorn, U.; Taake, C. Synthesis, X-ray diffraction and MAS NMR characteristics of nitrate cancrinite $Na_{7.6}[AlSiO_4]_6(NO_3)_{1.6}(H_2O)_2$. *J. Alloys Compd.* **2000,** *305*, 93-102.

(46) Bradbury, M. H.; Baeyens, B. A generalised sorption model for the concentration dependent uptake of caesium by argillaceous rocks. *J. Contam. Hydrol.* **2000,** *42*, 141-163.

(47) Rajec, P.; Shaw, G. Sorption of radiocesium on soils in the presence of electrolytes. *J. Radioanal. Nucl. Chem.-Artic.* **1994,** *183*, 147-157.

(48) Wampler, J. M.; Krogstad, E. J.; Elliott, W. C.; Kahn, B.; Kaplan, D. I. Long-term selective retention of natural Cs and Rb by highly weathered coastal plain soils. *Environ. Sci. Technol. 46*, 3837-3843.

(49) Um, W.; Serne, R. J.; Yabusaki, S. B.; Owen, A. T. Enhanced radionuclide immobilization and flow path modifications by dissolution and secondary precipitates. *J. Environ. Qual.* **2005,** *34*, 1404-1414.

(50) Zwingmann, N.; Mackinnon, I. D. R.; Gilkes, R. J. Use of a zeolite synthesised from alkali treated kaolin as a K fertiliser: Glasshouse experiments on leaching and uptake of K by wheat plants in sandy soil. *Appl. Clay Sci.* **2011,** *53*, 684-690.

(51) Suwardi; Goto, I.; Ninaki, M. The quality of natural zeolites from Japan and Indonesia and their application effects for soil amendment. *Journal of Agricultural Science Tokyo Nogyo Daigaku* **1994,** *39*, 133-148.

(52) Ming, D. W.; Allen, E. R. Use of natural zeolites in agronomy, horticulture, and environmental soil remediation. *Natural Zeolites: Occurrence, Properties, Applications* **2001,** *45*, 619-654.

(53) Shrivastava, O. P.; Komarneni, S. Cesium selectivity of (Al+Na)-substituted tobermorite. *Cem. Concr. Res.* **1994,** *24*, 573-579.

APPENDIX A

Texture, specific surface area (SSA) and cationic exchange capacity (CEC) of the unreacted and the reacted Hanford sediment (standard deviations in subscript). Table from Perdrial et al (6).

Sample name	Particle size distribution ($g.kg^{-1}$)[a]			SSA_{ext}[b]	CEC[c]
	Sand	Silt	Clay	$m^2.g^{-1}$	$mmol_c.kg^{-1}$
Hanford sediment[d]	$802.57_{1.83}$	$167.75_{1.54}$	$29.75_{0.37}$	$12.33_{0.05}$	$87.94_{2.52}$
6mo $HIGH_{[+CO2]}$	$736.70_{2.63}$	$217.40_{2.17}$	$45.93_{0.48}$	$8.88_{0.04}$	$58.17_{1.27}$
6mo $HIGH_{[-CO2]}$	$699.33_{1.20}$	$240.17_{0.81}$	$60.50_{0.46}$	$8.35_{0.04}$	$53.70_{2.48}$
6mo $LOW_{[+CO2]}$	$662.00_{10.82}$	$289.13_{9.10}$	$48.87_{1.73}$	$9.33_{0.06}$	$75.02_{0.04}$
6mo $LOW_{[-CO2]}$	$637.33_{15.30}$	$308.43_{11.41}$	$54.23_{3.90}$	$9.49_{0.09}$	$59.40_{1.40}$
12mo $HIGH_{[+CO2]}$	$670.70_{12.75}$	$271.80_{9.95}$	$57.57_{4.82}$	$8.90_{0.01}$	$56.19_{0.56}$
12mo $HIGH_{[-CO2]}$	$716.23_{9.74}$	$227.17_{7.08}$	$56.50_{2.06}$	$8.90_{0.06}$	$55.16_{2.66}$
12mo $LOW_{[+CO2]}$	$591.67_{15.43}$	$352.27_{13.08}$	$56.07_{2.37}$	$9.72_{0.09}$	$65.92_{0.03}$
12mo $LOW_{[-CO2]}$	$575.76_{24.81}$	$358.05_{18.88}$	$66.20_{5.93}$	$10.94_{0.12}$	$50.93_{1.49}$

[a] Particle size distribution measured by laser diffraction granulometry.

[b] Total specific surface area measured by N_2(g) adsorption.

[c] CEC measured using the Cohex exchange method.

[d] Values from Thompson et al. (14)

APPENDIX B

Element release from the 6-month LOW treatments.

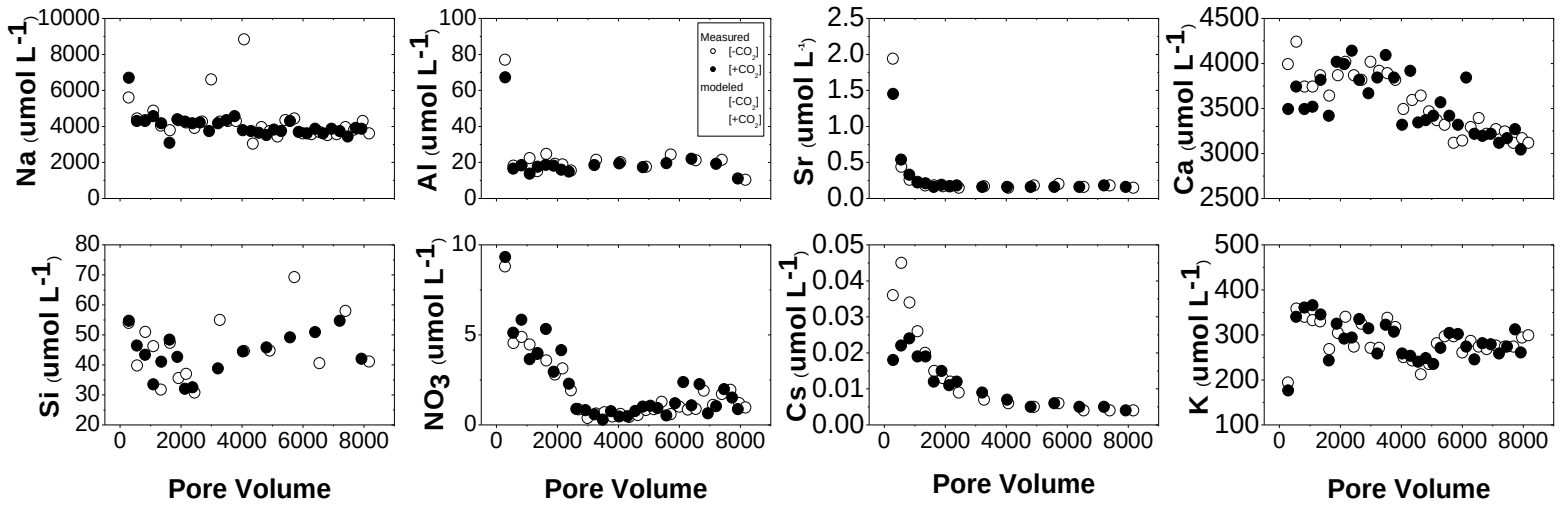

APPENDIX C

Element release from the 6-month HIGH treatments.

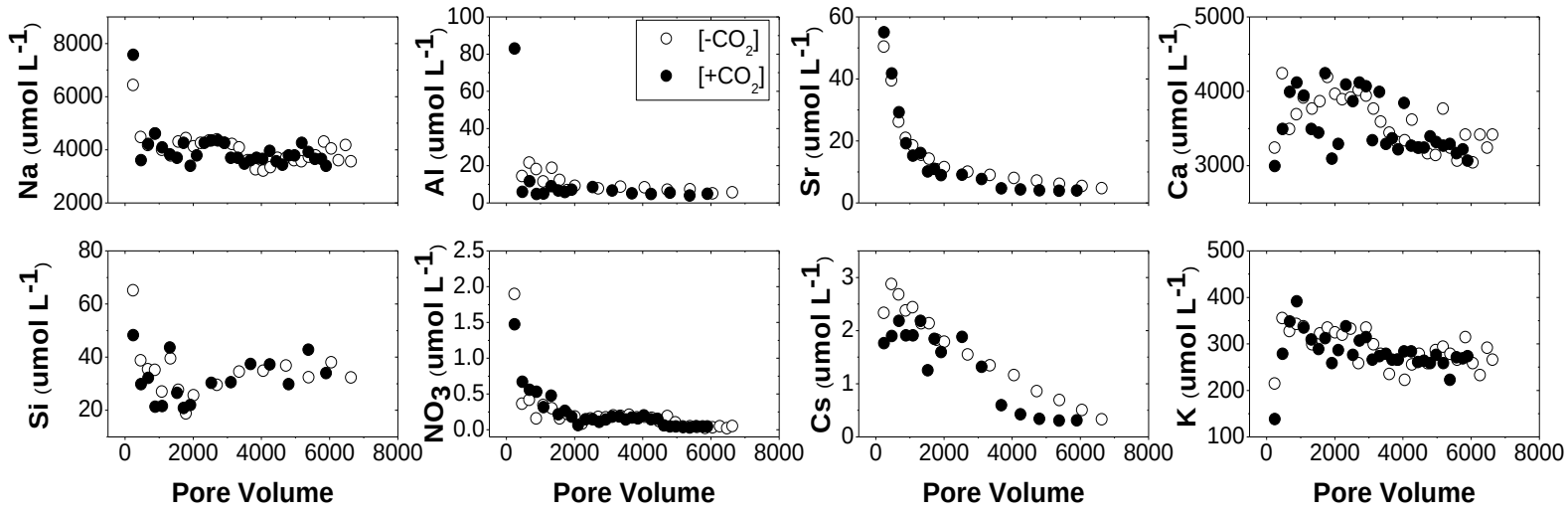

APPENDIX D

The images of field emission scanning electron microscopy (FE-SEM) and energy-dispersive spectrometry (EDS-spectra) of pristine Hanford sediments and the sediments saturated with Cs^+, K^+ and H^+.

FE-SEM images in this research serve as supporting material. We expected to visually assess the FES of pristine Hanford sediments, which were saturated by Cs^+, K^+ or H^+. We prepared samples with individual saturation of CsCl, KCl, or HCl. Approximately 0.18 g pristine Hanford sediments was added into 2-mL centrifuge tubes with 0.1 M CsCl. The samples were shaken for 20 minutes, and centrifuged (14,000 rpm, 30 min) to obtain the particle fraction < 0.03 μm in the supernatants. The supernatants were frozen and freeze-dried for 24 h. Then, the samples were re-suspended in 0.1 M CsCl, shaken for 20 min, frozen, and freeze-dried for 24 h again. This saturation (wet-dry) procedure was repeated two times in order to enhance the sorption of Cs on FES. Then, the samples were saturated with 18.2 MΩ water and put into dialysis membrane until the EC value of the solution was stable. This step was for reducing the extra salt. Finally, the samples were freeze-dried for FE-SEM analysis (JSM-7001F). The saturation with KCl and HCl followed the same procedure. The results show that compared to the image of pristine Hanford sediments, the images of treatments with H^+ saturation showed that the materials were dissolving. The results of EDS-spectra showed the dissolution of Fe, Mg, and Ca. The images of the K^+ saturation treatment

appeared to be coated materials and the EDS spectra showed the increase of K, Fe, and Al and the decrease of C and Mg. Finally, the images of the Cs^+ saturation treatment still showed fibrous materials similar to the untreated Hanford sediments. However, the EDS spectra showed the appearance of Cl and Cs and the dissolution of Ca.

The FE-SEM image of the pristine Hanford sediments.

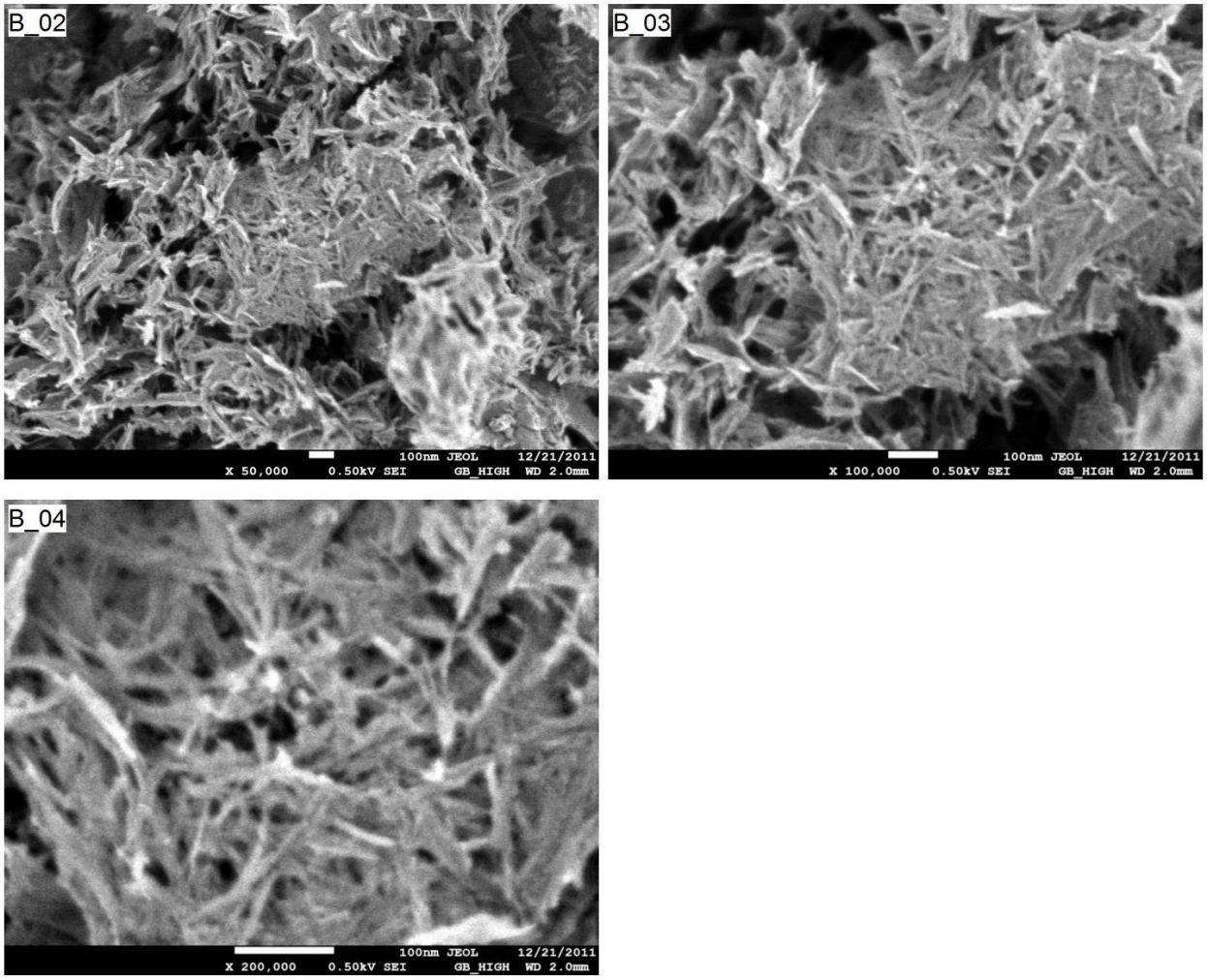

The EDS-spectra of the pristine Hanford sediments.

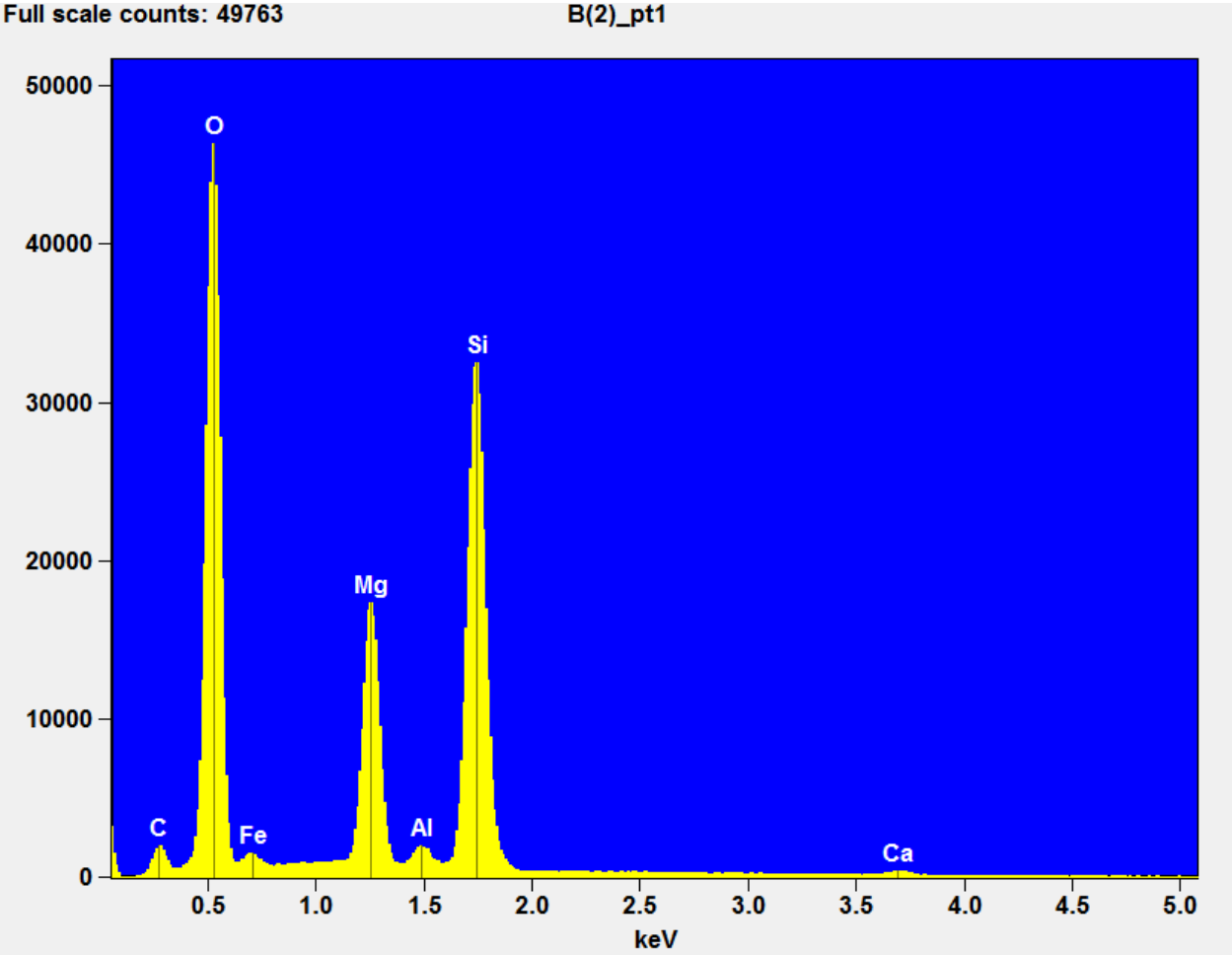

The FE-SEM image of Hanford sediments with 0.1 M HCl saturation.

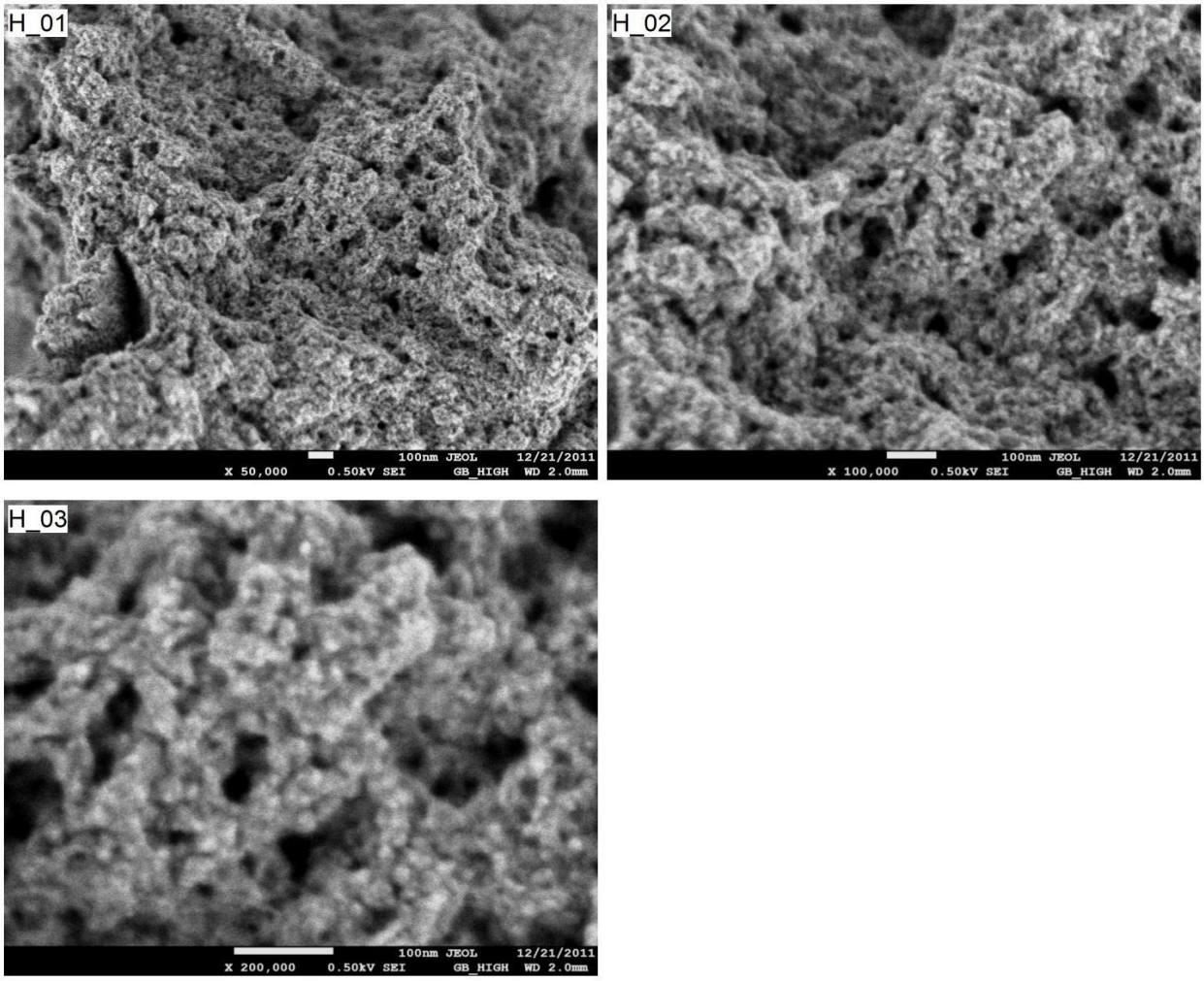

The EDS-spectra image of Hanford sediments with 0.1 M HCl saturation.

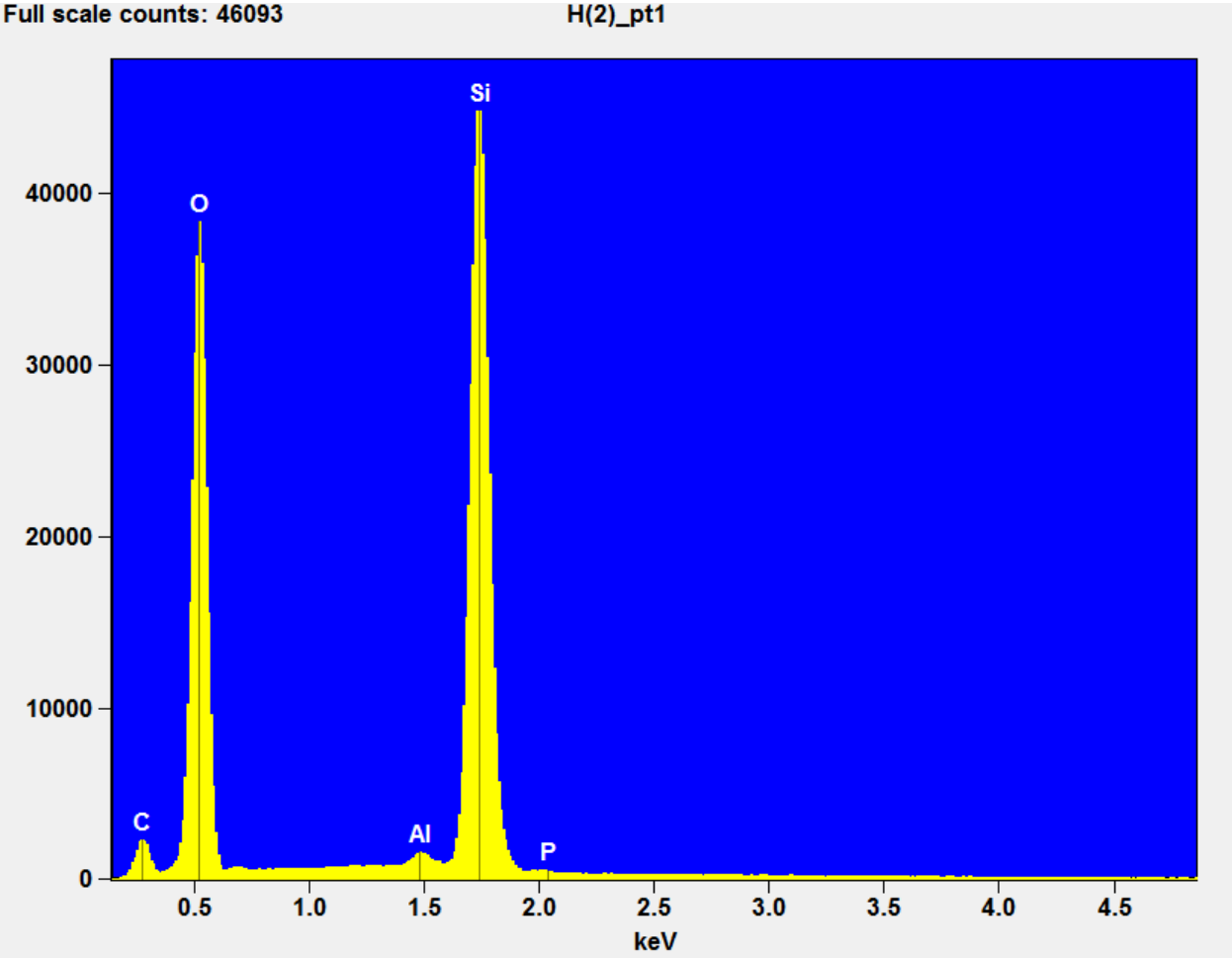

The FE-SEM image of Hanford sediments with 0.1 M KCl saturation.

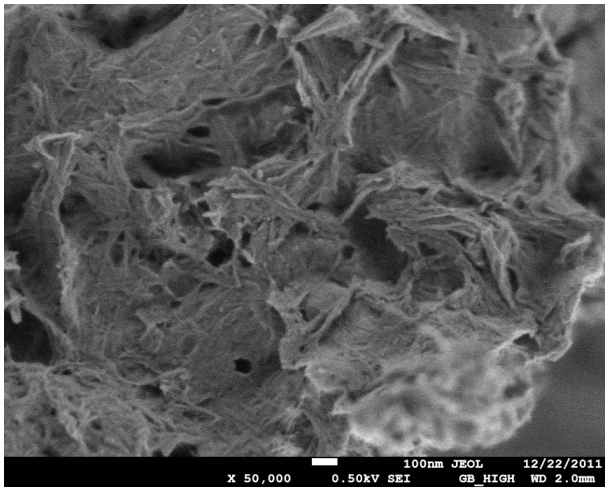

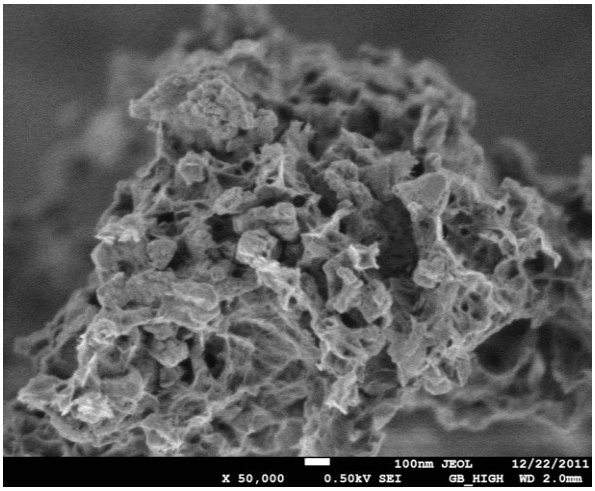

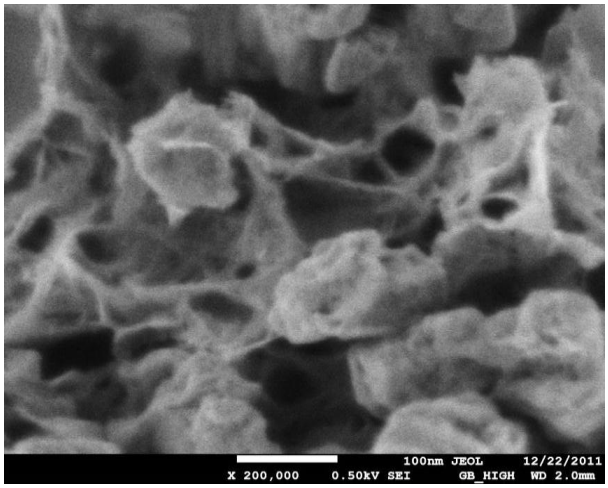

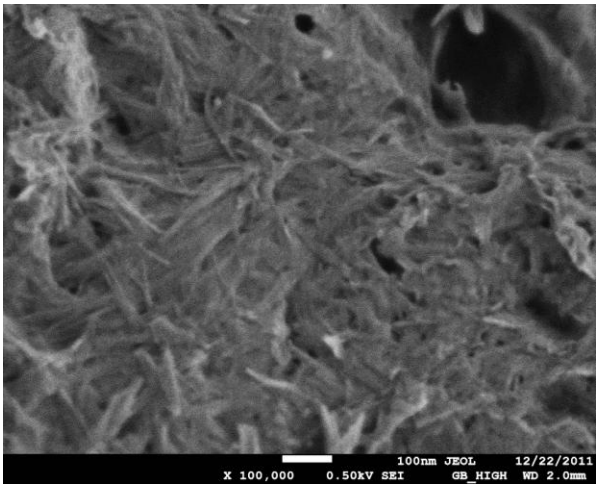

The EDS-spectra image of Hanford sediments with 0.1 M KCl saturation.

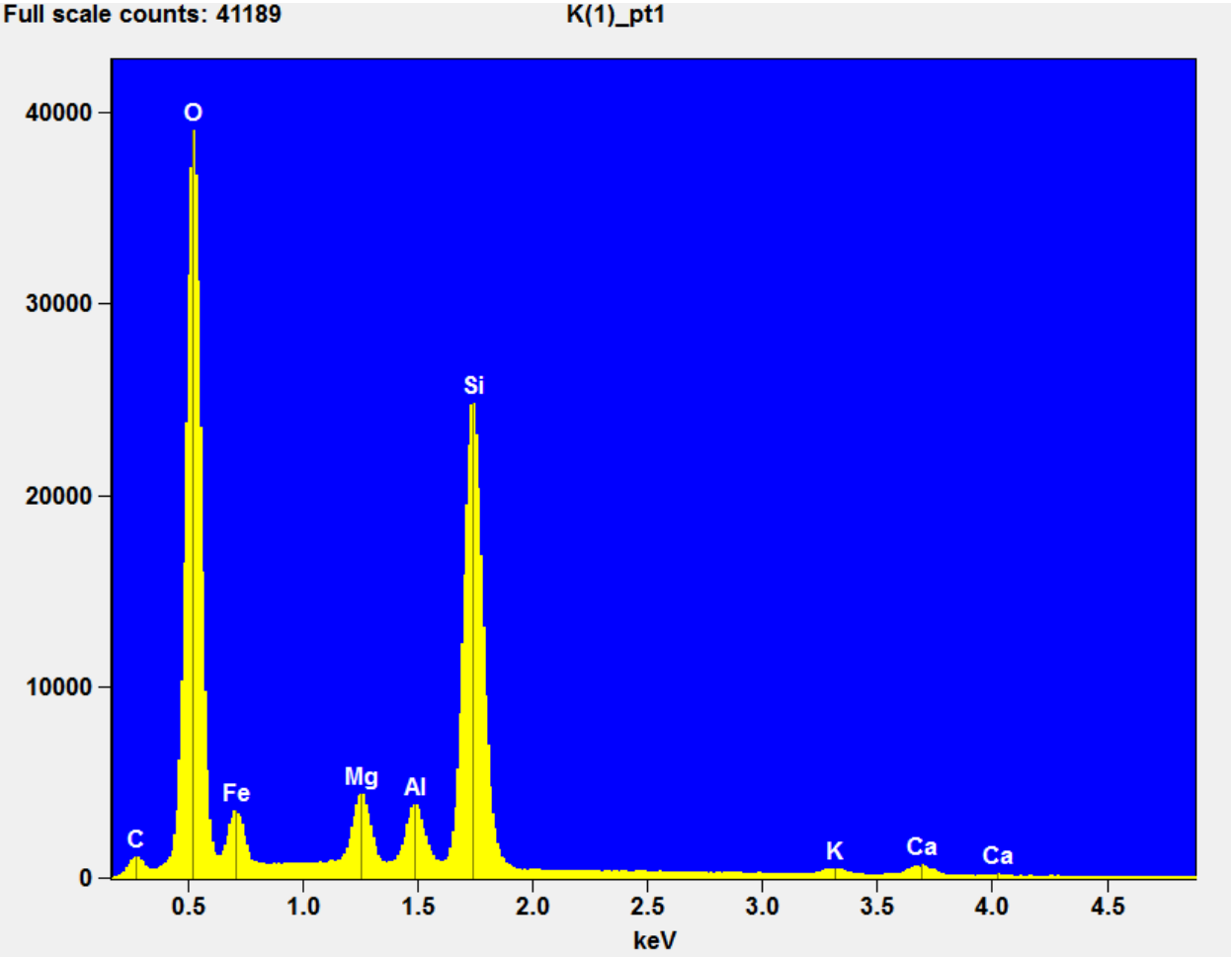

The FE-SEM image of Hanford sediments with 0.1 M CsCl saturation.

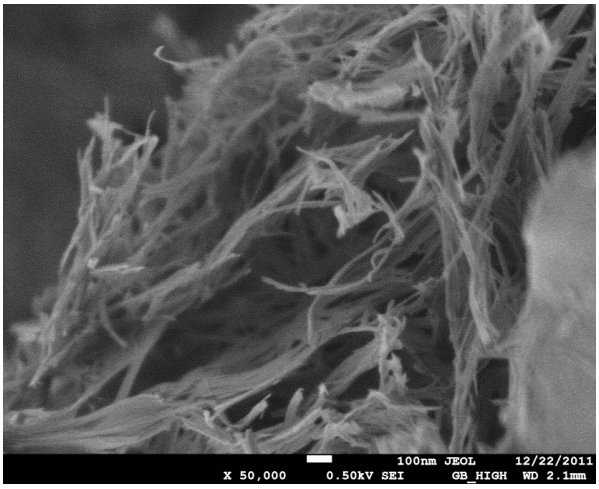

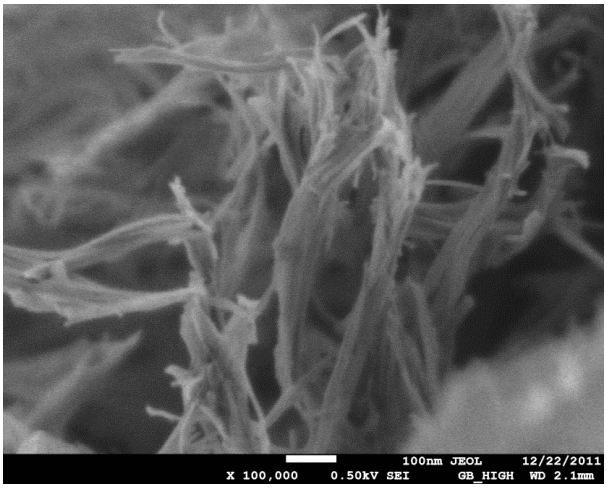

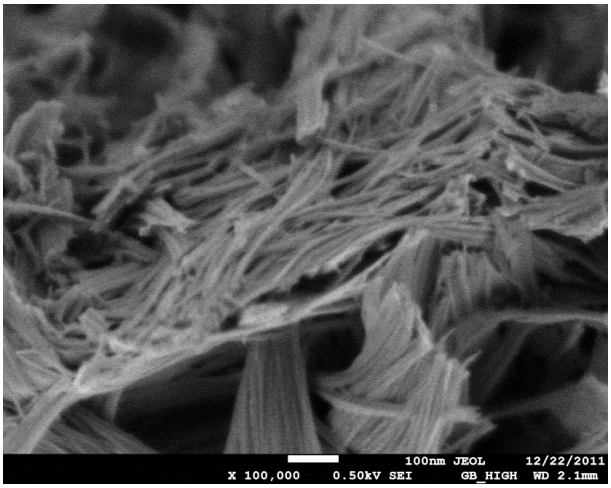

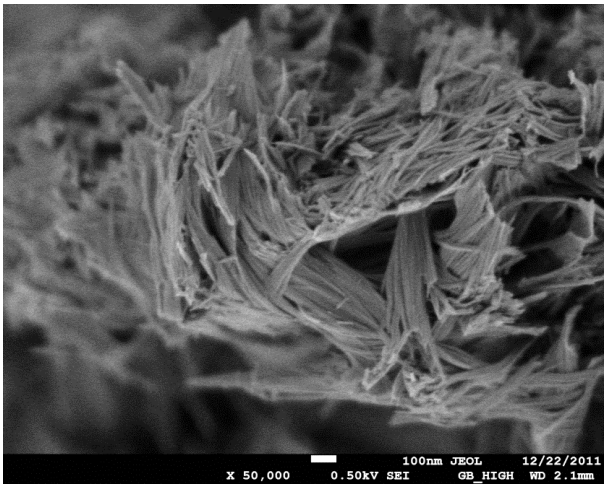

The EDS-spectra image of Hanford sediments with 0.1 M CsCl saturation.